DVB-H Antenna in a Small Handheld Device

Group No. 1121

Zena Fourzoli
Radwan Charafeddine

February-June 2007

Aalborg University

Aalborg University
E-Studyboard
Mobile Communications 10th semester

TITLE:

DVB-H antenna in a small handheld device

THEME:

Mobile Communications

PROJECT PERIOD:

February 2007 - June 2007

PROJECT GROUP:
07gr1121

GROUP MEMBERS:
Zena Fourzoli
Radwan Charafeddine

SUPERVISOR:
Gert F. Pedersen

Number Of Duplicates: 2

Number Of Pages In Report: 58

Number Of Pages In Appendix: 24

Total Number Of Pages: 82 (without Matlab code)

Abstract
Digital Video Broadcasting for Handheld devices (DVB-H) is a technical specification for bringing broadcast services to handheld receivers. It will be possible to watch TV mobile devices such as mobile phones. However, since the typical size of a mobile phone is small compared to the wavelength of the transmitted DVB-H signals ($\lambda = 50$cm for the central frequency), designing the internal antenna is very challenging.
In this Master Thesis we focused our attention on internal tuneable antennas that we simulated using FDTD technique. We investigated the previous work done on DVB-H antennas as a starting point. It appeared that the use of matching circuits was necessary to cover the whole band of interest to have a good trade-off between the antenna size and its performances. However, simple matching techniques such as L networks were not efficient enough. This is why we focused on broadband matching technique. We used a simple wire as antenna and improved its performances using Chebyshev matching filters. The whole DVB-H band has been covered using less than half the number of previously used matching circuits. This improved consequently the performances while minimizing the total losses.

Contents

List of Figures

List of Tables

Abbreviations

4K-mode 4096 carriers in one OFDM symbol

AR Autoregressive

BER Bit Error Rate

CSI Channel State Information

DVB-H Digital Video Broadcasting for Handheld devices

DVB-T Digital Video Broadcasting-Terrestrial

FDTD Finite-Difference Time-Difference

FM Frequency Modulation

FFT Fast Fourier Transform

GSM Global System for Mobile Communication

ICI Inter Carrier Interference

IFA Inverted-F Antenna

ISI Inter Symbol Interference

MEMS Micro-Electro-Mechanical Systems

MPE-FEC Foward Error Correction for Multiprotocol Encapsulation

OFDM Orthogonal Frequency Division Multiplexing

PIFA Planar Inverted F Antenna

PIN Positive intrinsic negative

PLR Packet Loss Ratio

PSI Program Specific Information

SAR Specific Absorption Rate

SI System Information

SFN Single Frequency Network

TDM Time Division Multiplexing

TPS Transmission Parameter Signalling

TS Transport Stream

List of symbols

All the symbols we used in this master thesis are listed below:

$2k$: 2048 OFDM carriers
$4k$: 4096 OFDM carriers
$8k$: 8192 OFDM carriers
λ : Wavelength at center frequency
T_{OFDM} : OFDM symbol duration
r : Sphere radius
k : Wavenumber
η_{rad} : Radiation efficiency
P_{rad}: Radiated power
P_{in} : Power accepted by the antenna
D : Directivity
G : Gain
Z_0 : Characteristic impedance of a transmission line
Z : Impedance of the load
ρ : Reflection coefficient
P_t : Incident power to the load
P_{in} : Power accepted by the load
P_{rad} : Power radiated by the load
S_{11} : Scattering parameter
L_{refl} : Reflection loss
L_{retn} : Return loss
B_r : Relative bandwidth
BW_{abs} : Absolute frequency bandwidth
CF : Arithmetic center frequency of the impedance band
G : Conductance (in a resonator circuit model)
C : Capacitance (in a resonator circuit model)
L : Inductance (in a resonator circuit model)
Y_0 : Admittance of a transmission line (in a resonator circuit model)
P_l : Average power loss(in a resonator circuit model)
V : Peak value of the voltage across the components (in a resonator circuit model)
I : Current flowing through the inductance L (in a resonator circuit model)
W_c : Average energy stored in the capacitance C in a resonator circuit model)
W_i : Average energy stored in the inductance L in a resonator circuit model)
W : Total energy stored in the circuit in a resonator circuit model)
f_r : Resonant frequency
ω_r : Angular resonant frequency

P_{in} : Losses in the resonator structure
Q_0 : Unloaded quality factor
Q_{rad} : Radiation quality factor
P_d : Losses in dielectrics
P_c : Losses in conductors
Q_d : Dielectric quality factor
Q_c : Conductor quality factor
S : Voltage standing wave ratio
T : Coupling coefficient for a parallel resonant circuit
λ_0 : Free space wavelength
ω_{norm} : Normalized pulsation (for Chebyshev frequency filter design)
ω : Pulsation ($\omega = 2\pi f$)
ω_c : Cut-off pulsation
$C_n^2(\omega)$: nth-order Chebyshev polynomial of the first kind
ε : Ripple factor that gives a magnitude equal to $\frac{1}{\sqrt{1+\varepsilon^2}}$
H_0 : Constant
α_p : Passband ripple
α_s : Stop band attenuation
ω_p : Cut-off frequency
ω_s : Stopband frequency
ω_{s-norm} : Normalized stopband pulsation
ω_{p-norm} : Normalized passband pulsation
s : Lowpass frequency
S : Bandpass complex frequency
ω_0 : Center frequency of the bandpass filter
B : Bandwidth of the bandpass filter
$H(j\omega)$: Transfer function
R_a : Real part of the antenna impedance
δ : The decrement
$g_{k|_{k=1ton}}$: Inductance of a series coil, or the capacitance of a shunt capacitor
L_{Ar} : Passband ripple loss

Acknowledgment

The work on this thesis has been a challenging and always interesting experience.

We would like to express our gratitude to our supervisor Gert Frolund Pedersen for his valuable guidance throughout this project and all those people who directly or indirectly helped us to realize this project, especially Mauro Pelosi for the help he provided to us.

We also wish to thank our respective families for their encouragement. We express our full gratitude to our respective parents: thanks to their support we have been able to spend a whole year in Denmark allowing us to study in the Department of Mobile Communications at Aalborg University. We dedicate to them our Master-thesis.

Zena Fourzoli

Radwan Charafeddine

Chapter 1

Introduction

1.1 Overview

The demand for compact mobile telephone handsets has grown over the years. More recently new services have been incorporated in our mobile phones such as the possibility to listen to music or to the radio, to play games and to take pictures. Watching television on a mobile terminal will be the next step in the deployment of services on mobile terminals.

Digital Video Broadcasting for Handheld devices (DVB-H) is a technical specification for bringing broadcast services to handheld receivers. DVB-H technology adapts the Digital Video Broadcasting-Terrestrial (DVB-T) system to the specific requirements of handheld, battery-powered receivers. The whole system should provide a good reception in all situations, a good picture quality and a limited impact on phone battery life. The space available in nowadays small phones is very limited because of the batteries' size, the space taken by the antennas (Global System for Mobile Communication (GSM), Bluetooth, radio) and the screen.

1.2 Problem description

The typical size of a mobile phone (100*40*10 mm^3) is small compared to the wavelength of the transmitted DVB-H signals (λ = 50 cm at center frequency 600 Mhz). Designing an internal antenna for watching television on a mobile terminal is very challenging for 3 reasons:

1. the space available in mobiles is very small (less than 3 cm^3)
2. the wavelength
3. and the bandwidth to cover

In this master-thesis we will focus on internal tuneable DVB-H antenna that can be implemented in a handheld device. Thus we will investigate the main requirements for the DVB-H antenna to be as small as possible. We will assume that :

1. the antenna volume must be inferior to 3 cm^3
2. the chassis box is 80*40*8 mm^3
3. the covered band must be from 470 Mhz to 730 Mhz

Different types of antennas and techniques will be investigated.

1.3 Organization of the report

The report is organized as follows. Some general information about background knowledge such as DVB-H, small antennas, Planar Inverted F Antenna (PIFA), Finite-Difference Time-Difference (FDTD) technique, switching circuits, is explained in details in Chapter 2. In chapter 3, the previous work that has been done on DVB-H antenna for small handheld device is presented with some results. Chapter 4 describes the improvement brought to the preliminary work using Chebyshev impedance matching technique and the results we obtained. The phone position is discussed in chapter 5. Finally Chapter 6 draws the conclusion and gives directions for future works.

Chapter 2

Background

2.1 DVB-H

DVB-T was launched in order to receive the television at home in high quality. But it is still impossible for us to watch the news in the subways, or in the car on our cell phone. Why? Simply because the technologies were not adapted to small portable devices:

1. The power consumption of the receiver had to be reduced: in our case, time slicing provides it.
2. The antenna size had to be small enough to be integrated in mobile phones.

The operators are offering TV services on 3G; but one of the main problematic at the operator side is to minimize the maximum the network costs and bandwidth costs. This is why DVB-H is the answer. This technology in parallel with the cellular network will broadcast any type of data. The main advantage of such a network is that it avoids the connected mode used in traditional GSM and so limits the network costs. In the user side, DVB-H works in the same way as traditional Frequency Modulation (FM) radio; it only has to switch from one channel to another. DVB-H offers a downlink canal that can achieve a data rate of 10 Mbps. The figure 2.1 shows how a DVB-H network could be considered in parallel with the GSM network.

Table 2.1 presents different characteristics between DVB-H and DVB-T.

2.1.1 DVB-H main parameters

DVB-H combines the following elements in the link layer and physical layer:

- Link layer:
  - Time Slicing to reduce the power consumption and in-depth interleavers.
  - Foward Error Correction for Multiprotocol Encapsulation (MPE-FEC) to reduce the Bit Error Rate (BER).
- Physical layer:
  - Transmission Parameter Signalling (TPS) bits signaling for discovery with the cell identifier.

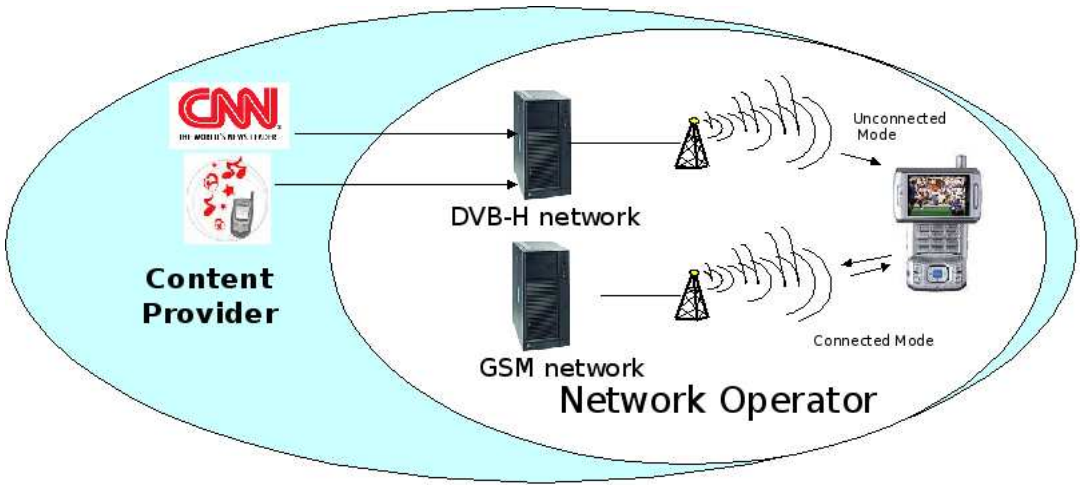

Figure 2.1: DVB-H network

– 4096 carriers in one OFDM symbol (4K-mode) which is a good trade-off between mobility and Single Frequency Network (SFN) cell size.

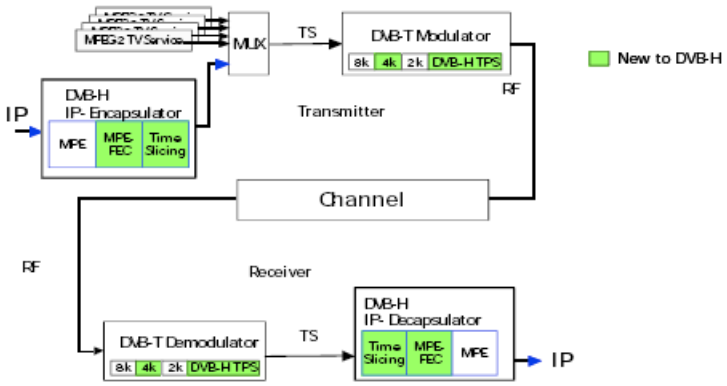

Figure 2.2: DVB-H infrastructure
[11]

2.1.2 Link layer parameters

Time slicing

Because DVB transmission usually provides 10 Mbps bitrate, it is possible to use Time Division Multiplexing (TDM). The main function of time slicing is to send the data using a higher bitrate in less time compared to the bitrate that would be used if the data were sent using traditional streaming mechanisms. It is done in a way that the mobile station doesn't need to stay ON all the time. The figures 2.3, 2.4 and 2.5 illustrate how the data are sent in the burst: respectively traditional streaming, Time Slicing at the emitter and Time Slicing at the receiver. Depending on the channel we want to watch, the mobile will be synchronised on one of these bursts.

Table 2.1: DVB-T and DVB-H parameters [5]

	DVB-T	DVB-H
Frequency	174 to 230 MHz, 470 to 862 MHz	470 to (730 with GSM 900) 862 MHz - L-Band: 1452 to 1492 MHz
Modulation	QPSK, 16-QAM and 64-QAM	QPSK, 16-QAM, COFDM
Polarization	Horizontal	Vertical
ERP		50 kW to 80 kW
Channel Bandwidth	6/7/8 Mhz	5/6/7/8 MHz
Cell size	17 km (2K Mode), 67 km (8K Mode)	7 km (2K Mode), 33 km (4K Mode), 67 km (8K Mode)
Receiver equipment		Sagem MyX8, Nokia N92, PDA-based with HiCast receiver (DiBcom) [14]
Peak Data rate	4.98 Mbps to 31.67 Mbps	typ. 0.2 Mbps to 0.384 Mbps per segment
Power Reduction Method		Time Slicing
Source coding Video/Audio	MPEG-2	MPEG-4/H.264
Max Speed	up to 300 km/h	more than 300 km/h

During the off-time the receiver monitors neighbouring cells. Handover is required only when changing network in the case we are in a SFN: transmitters form one cell since they are emitting at the same frequency.

MPE-FEC

The DVB specifications suggest 4 data broadcast methods that are:

- Data piping
- Data streaming
- MPE (Multiprotocol Encapsulation)
- Carrousel

MPE is the most suitable for the delivery of streaming services. The figure 2.6 presents the protocol layers for DVB-H using MPE-FEC. MPE is located in the data link layer between the transport stream layer and the IP layer. This allows more flexibility to support any other network layer protocol.

The System Information (SI) and the Program Specific Information (PSI) tables are signaling data that are not time sliced. SI table contains :

- NIT information that is static and defines the network. The receiver accesses it once unless it changes network.

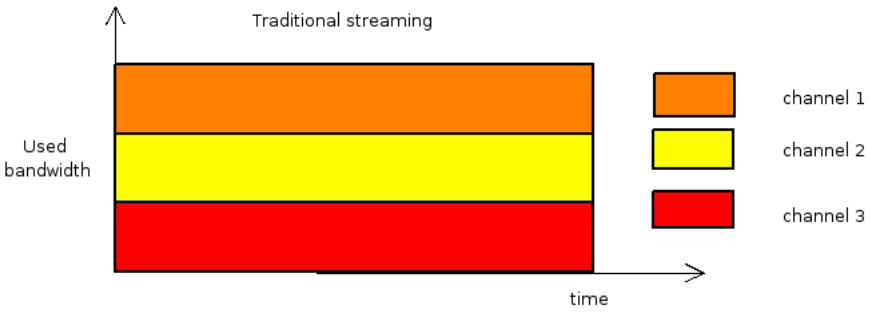

Figure 2.3: Traditional streaming concept

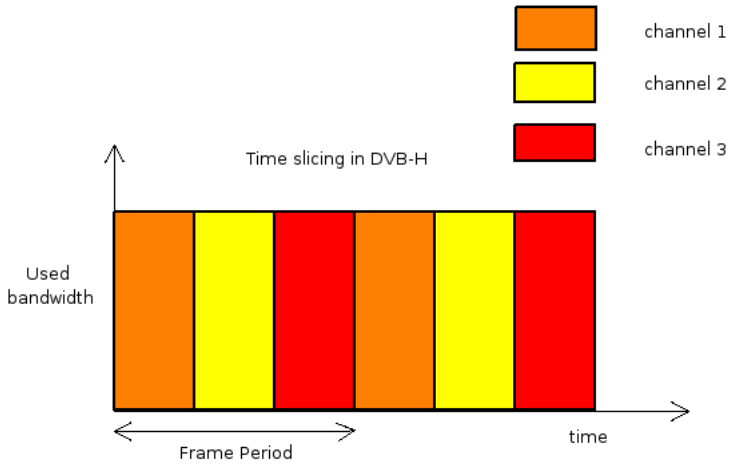

Figure 2.4: Time Slicing concept at emitter

- INT information contains the signaling concerning the different streams and is also used once unless the streams parameters change. In this case, the receiver will be informed by the PSI tables that are sent every 100 ms at least.

MPE is combined with FEC which enables parity data. This enables the receiver to rebuild error free IP datagram. Also, the Packet Loss Ratio (PLR) can decrease of about 10 percent when FEC represents 25 percent of the Transport Stream (TS) data. It is also possible to decrease the PLR combining different code rate and modulation. This method presents immunity to impulsive interference. The figure 2.7 presents MPE-FEC frame.

The frame is divided in two subframes:

- The figure 2.8 presents the MPE that is composed of 191 columns. The IP datagrams are put one after another. The left space is then padded with zero bytes.
- The figure 2.9 is for the FEC and is composed of 64 columns that make a total of 255 for the entire frame. Reed Solomon algorithm RS (255,191) is used in order to recover the datagram.

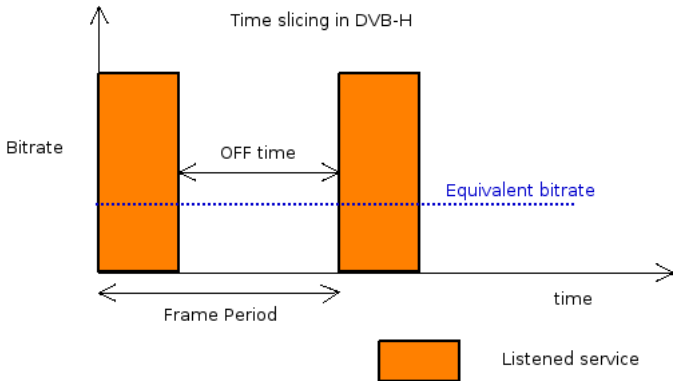

Figure 2.5: Time Slicing concept at receiver

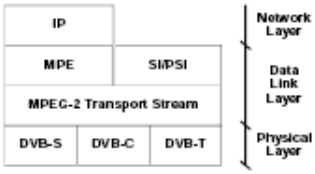

Figure 2.6: DVB-H Protocol Stack
[11]

Then the number of rows has to be defined from 1 to 1028.

2.1.3 Physical layer elements

4K-mode

The 4K-mode has been chosen because it is a good trade-off between spectrum efficiency, the reception performances and the power consumption. The 8K-mode is not adapted to mobility (requires Channel State Information (CSI)) while the 2K-mode is not spectral efficient. Usually in DVB-H, the used modulation is 16 QAM with a coding rate of $\frac{1}{2}$ or $\frac{2}{3}$;

TPS-bit

They are used in order to signal time slicing, MPE-FEC and 4k-mode options.

2.1.4 Other parameters used in DVB-H

OFDM transmissions:

DVB-T and DVB-H transmissions are based on Orthogonal Frequency Division Multiplexing (OFDM). The signal is sent into orthogonal subcarriers. The main objective of OFDM technique is to avoid the frequency selective fading, thus avoid the Inter Symbol Interference (ISI) in the receiver. It is done by dividing the whole system bandwidth with several subcarriers such that each subcarrier experiences flat fading only. Multicarrier transmission is a solution that solves this problem. It consists of dividing the bandwidth in multiple sub channels separated by a guard interval, and by the same way it increases the period size.

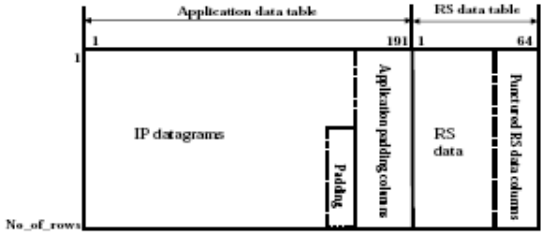

Figure 2.7: MPE-FEC frame
[11]

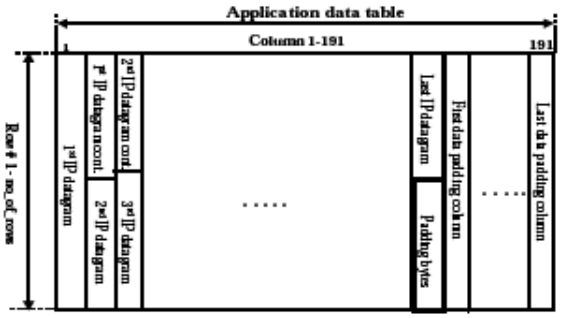

Figure 2.8: MPE subframe
[11]

The principles of multicarrier transmission are:

- Split the bandwidth in N narrowband subcarriers
- Parallel transmission of the N subcarriers, where OFDM symbol duration, $T_{OFDM} \gg \Delta\tau_{max}$
- Guard interval insertion in order to make it robust against ISI and Inter Carrier Interference (ICI).

DVB-H uses SFN. The emitter will work at the same frequency broadcasting the same signal at the same time.

In order to improve the quality of the video received, DVB-H uses a new codec called AVC/H264. This codec has been developped by the MPEG group and provides a better encoding of the video: it is possible to compress more data compared to the previous MPEG-2 codecs. This codec needs a lot of processing and the mobile equipment will need to be more powerful. It is also possible to broadcast using IPDATACAST other metadata and services such as the meteo or horoscopes.

DVB-H standards for antenna's receivers

The receivers should be able to get the frequency range from 470 MHz to 862 MHz. The method of implementation of the antenna is not specified in the standards. But because it

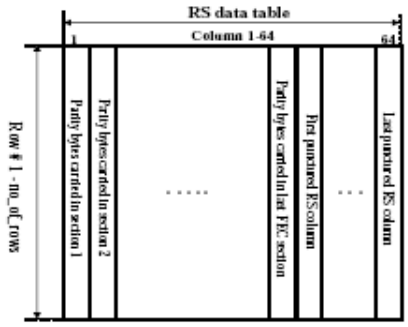

Figure 2.9: FEC subframe
[11]

needs to be small enough to fit into a small phone (80mm x 40mm x 8mm, for the length, the width and the thickness respectively), it makes the requirements very difficult to achieve.

Table 2.2 makes a summary of DVB-H parameters.

Table 2.2: DVB-H parameters [12]

	DVB-H with GSM900	DVB-H without GSM 900
Frequency	470 to 730 MHz	470 to 862 MHz
Channel Bandwidth	232 Mhz	392 MHz
Center frequency	586 MHz	666 MHz
Center frequency wavelengh	52 cm	45 cm

2.2 Small Antennas theory

The designer needs to make a trade-off between antenna size and performance as shown in figure 2.10. There is no limit in the number of variant that can be derived from a small number of generic types. An antenna can be defined as small in the following terms [9]:

1. electrically small : bounded by the sphere having a radius equal to $\frac{\lambda}{2\pi}$, where λ is the free space wavelength.
2. physically constrained : considerable size reduction in one plane.
3. functionally small: the performances of the antenna are increased compared to its size.
4. physically small: in relative sense.

An antenna is characterized by:

- its Q factor that is ratio of the energy stored in the antenna over the energy dissipated per radian of oscillation and is a function of the antenna size and the wavelength.

- its impedance characteristic Z composed by a real part which includes the radiation resistance and the radiation losses and an imaginary part called reactance.
- its efficiency which is the ratio of radiated power over the total input power.
- its impedance bandwidth which is the frequency of use of the antenna.

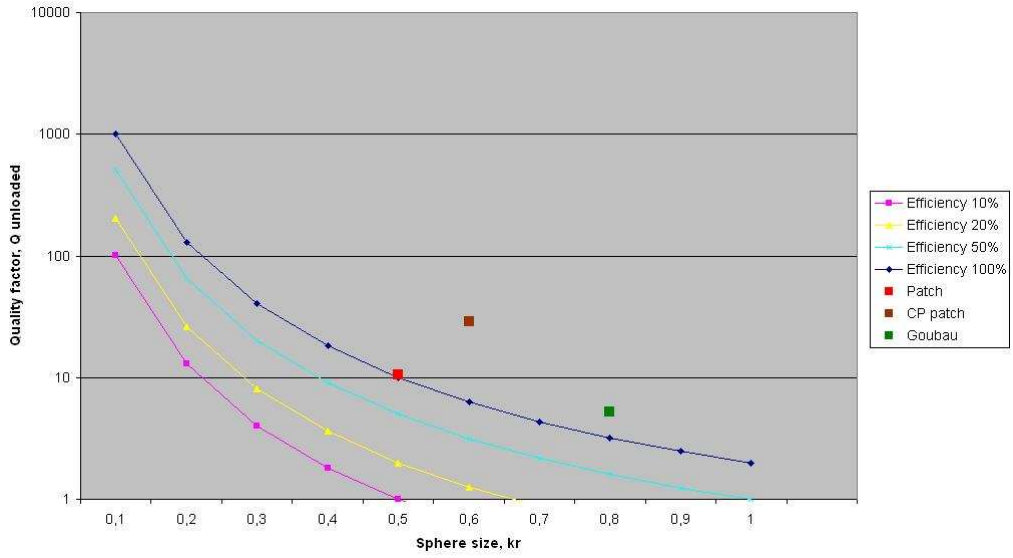

Figure 2.10: Trade-off between the Q factor and the efficiency

On figure 2.10 we placed some basic small antennas: these are the Goubau antenna, the Patch antenna and the Circular polarized patch antenna [21]:

1. Goubau antenna: radius r=7.58 cm, $\frac{r}{\lambda} = 0.14$
2. Patch antenna: radius r=14.61 mm, $\frac{r}{\lambda} = 0.093$
3. Circular polarized patch antenna: radius r=1.7 cm, $\frac{r}{\lambda} = 0.14$

With the previous data we found the value of λ in order to find the value of the wavenumber k and finally calculated the product kr to get the value of the quality factor. Actually on the figure 2.10 we have the bandwidth (expressed as a Q factor) against the size of the antennas expressed as the electrical circumference of the inscribing sphere. It has been established that for an electrically small antenna contained within a given volume, the antenna has an inherent minimum value of Q [24].

The Patch antenna and the Goubau antenna are antennas above the groundplane, so it is difficult to know exactly what radius of a sphere is required to contain the near fields. As a rule of thumb, the groundplane needs to be about a half-wavelength square for the impedance to be essentially independent of the groundplane size [21].

In the next sections we will see some important aspects related to small internal antennas and matching circuits.

Efficiency, directivity and gain

Radiation efficiency η_{rad} is defined as the ratio between the radiated power P_{rad} and the power accepted by the antenna P_{in} (see figure 2.11):

$$\eta_{rad} = \frac{P_{rad}}{P_{in}} \tag{2.1}$$

The directivity D and the gain G of an antenna are connected to each other by η_{rad} as:

$$G = \eta_{rad} D \tag{2.2}$$

Directivity describes the directional property of an antenna and the gain takes into account the losses in the antenna structure. For an ideal antenna the gain and the directivity are equal.

Matching circuits

Let's consider a circuit with a load (it can be an antenna) and a transmission line. If the impedance Z of the load differs from the characteristic impedance Z_0 of a transmission line, part of the voltage is reflected from the load, as shown in figure 2.11, where ρ is the reflection coefficient. P_t, P_{in} and P_{rad} are the (total) incident power to the load, the power accepted by the load and the power radiated by the load, respectively.

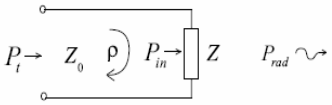

Figure 2.11: Voltage reflection from a mismatched load

The reflection coefficient is often denoted by the scattering parameter S_{11} and it can be calculated from [13]:

$$S_{11} = \frac{Z - Z_0}{Z + Z_0} \tag{2.3}$$

The load (e.g. an antenna) is matched, if the impedances of the load Z is equal to the conjugate of the characteristic impedance Z_0 of the transmission line. If this is not the case, only a part of the power will be transmitted to the transmission line and the rest of the power will be lost. A reflected wave will be created in the line due to the reflection caused by mismatching. Because of the reflection, a voltage standing wave is created along the transmission line. The voltage standing wave ratio $VSWR$ is defined as the ratio between the maximum and minimum voltages, so it can be calculated from [13]:

$$VSWR = \frac{1 + |\rho|}{1 - |\rho|} \tag{2.4}$$

The reflection is unwanted because the part of the power is not delivered into the load. It is a basic task in radio engineering, called impedance matching, to prevent the reflections. Power loss due to the reflection, called reflection loss L_{refl}, can be calculated from [13]:

$$L_{refl} = 10 \log \frac{1}{1 - |\rho|^2} \tag{2.5}$$

Return loss describes the ratio between the propagated and reflected power [13]:

$$L_{retn} = 10 \log \frac{1}{|\rho|^2} \tag{2.6}$$

Impedance bandwidth is defined as a frequency band over which a defined criterion is fulfilled. Normally the impedance bandwidth is defined in terms of the absolute value of the reflection coefficient ρ, return loss L_{retn} or voltage standing wave criterion $VSWR$.

The bandwidth BW_{abs} is defined by the absolute value of the reflection coefficient $|\rho| \leq -6$ dB, which corresponds to the return loss criterion of $L_{retn} \geq 6$ dB.

Relative bandwidth is defined according to the following equation:

$$B_r = \frac{BW_{abs}}{CF} \tag{2.7}$$

where BW_{abs} is the absolute frequency bandwidth and CF is the arithmetic center frequency of the impedance band.

In Appendix D we will study impedance matching network solutions, which is a part of the larger design process for a microwave component. The main idea of impedance matching is to place between the load impedance and the transmission line a matching network in order to avoid power losses. These power losses are undesired because we want to get the maximum power at the receiver side.

Resonant circuit and Quality factor of resonator

Reactive near-fields of a small antenna create a dominating reactive component in the impedance:

- The quality factor of the antenna is high
- The reactive component must be eliminated for matching

For very small antennas the reactive component must be compensated with matching opposite reactive component. Most small antennas can be made self-resonant, i.e. the reactance is nearly zero at center frequency. Close to resonance the antenna can be described with single or multiple lumped resonant circuits [15]. In small antennas, the reactive near fields are dominant and they store much more energy compared to the radiated fields. The resonance is achieved when the reactive energy is canceled out. It is advantageous to use the well-known resonator theory when analyzing small antennas. The figure 2.12 shows how a resonator can be modeled with a parallel resonance circuit. In that figure, G is the conductance, C is the capacitance and L is the inductance. Y_0 is the admittance of a transmission line. V is the peak value of the voltage across the components and I is the current flowing through the inductance L.

The conductance G models the losses P_l inside the resonator structure and then, the average power loss in the circuit is:

$$P_l = \frac{G|V|^2}{2} \tag{2.8}$$

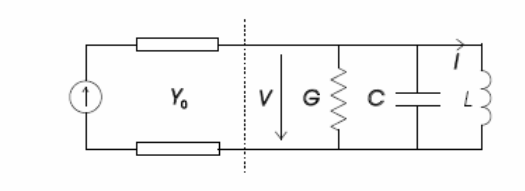

Figure 2.12: Resonator circuit model

The average energy stored in the capacitance C is:

$$W_c = \frac{C|V|^2}{4} \tag{2.9}$$

The average energy stored in the inductance L is:

$$W_i = \frac{L|I|^2}{4} \tag{2.10}$$

The total energy stored in the circuit is then $W = W_c + W_i$. The resonance is achieved when the energies of the capacitance C and the inductance L are equal. The resonant frequency f_r is then:

$$f_r = \frac{1}{2\pi\sqrt{LC}} \tag{2.11}$$

The quality factor Q describes the ratio between the energy stored and the power losses in a resonator structure. It can be defined as:

$$Q = \frac{w_r W}{P_l}, \tag{2.12}$$

where w_r is the angular resonant frequency which is defined by $w_r = 2\pi f_r$.

Using the previous definitions of the conductance, the average energy stored in the capacitance and the average energy stored in the inductance, we can derive the following equation for the quality factor in the equivalent circuit of the resonator:

$$Q = \frac{w_r W}{P_l} = \frac{w_r C|V|^2/2}{G|V|^2/2} = \frac{w_r C}{G} = \frac{1}{G w_r L} \tag{2.13}$$

Antenna quality factor

The antenna quality factor comprises:

$$\frac{1}{Q_0} = \frac{1}{Q_{rad}} + \frac{1}{Q_d} + \frac{1}{Q_c} \tag{2.14}$$

Each term represents some loss mechanism [15]:

1. Unloaded quality factor Q_0 includes all the losses P_{in} in the resonator structure.
2. Radiation quality factor Q_{rad} includes only radiation losses P_{rad}.
3. In an ideal case, the unloaded and radiation quality factors are equal but in practice there are losses in dielectrics P_d and conductors P_c, which are included in the dielectric quality factor Q_d and the conductor quality factor Q_c.

For purely antenna losses, the power dissipated in the metallic parts should be calculated from the surface current estimate and the surface resistivity. For dielectric parts, such as in patch antennas, the dielectric ohmic losses are calculated from the electric field estimates and the imaginary part of the dielectric constant [21].

Relation between bandwidth and quality factor

Impedance matching limits the bandwidth of a resonator [16]. To determine the bandwidth potential of an antenna we need the unloaded quality factor Q_0. The following connection can be established between the relative bandwidth B_r and the unloaded quality factor Q_0 of a resonator [17]:

$$B_r = \frac{1}{Q_0}\sqrt{\frac{(TS-1)(S-T)}{S}}, \tag{2.15}$$

where S stands for the $VSWR$, T is the coupling coefficient for a parallel resonant circuit, $T = Y_0/G$, where G is the conductance seen at the input of a resonator at the resonance frequency and Y_0 is the characteristic admittance of the transmission line. If we modify the value of the coupling coefficient T, then it is possible to modify the value of the relative bandwidth B_r (increase or decrease it). One can also increase the relative bandwidth B_r by lowering the unloaded quality factor Q_0 which means by increasing the losses P_{in} in the resonator structure.

Ultimate Bound on Radiation quality factor VS Antenna Size

The fields of an antenna can exactly be described by a serie of spherical field modes. By investigating the energy and modes it is possible to calculate a lower limit for the radiation quality factor of a single mode antenna closed inside a sphere with radius r [15]:

$$Q_{rad} = \frac{1}{kr} + \frac{1}{(kr)^3}, \tag{2.16}$$

where k is the wave number $2\pi/\lambda_0$, λ_0 is the free space wavelength at the used frequency. For small antennas the impedance bandwidth is approximately proportional to the electric volume (i.e. in wavelengths).

2.3 PIFA

PIFA can be considered as a kind of linear Inverted-F Antenna (IFA) where the wire radiator element has been replaced by a plate in order to expand the bandwidth. So before explaining what a PIFA is, let us see briefly what an IFA is.

The IFA is mainly composed of a wire element which is located above a ground plane, a short circuiting plate or pin, and a feeding mechanism for the planar element. The resulting antenna geometry looks like the letter F, rotated to face the ground plane. The excitation of currents in the ground plane is due to the excitation of currents in the IFA [1]. Thus we get an electromagnetic field thanks to the interaction of the IFA and an image of itself below the ground plane. We must keep in mind that the main role of an antenna is to transform the electrical signals into electromagnetic waves.

Now let us focus on the PIFA.

PIFA is the most used internal antenna and is suitable for the integration in handheld devices. Moreover the PIFA is easy to design for dual band [8].

As we have just said before, the thin wire horizontal segment is replaced by a flat conducting plate oriented parallel to the ground plane. The result is the PIFA shown in figure 2.13.

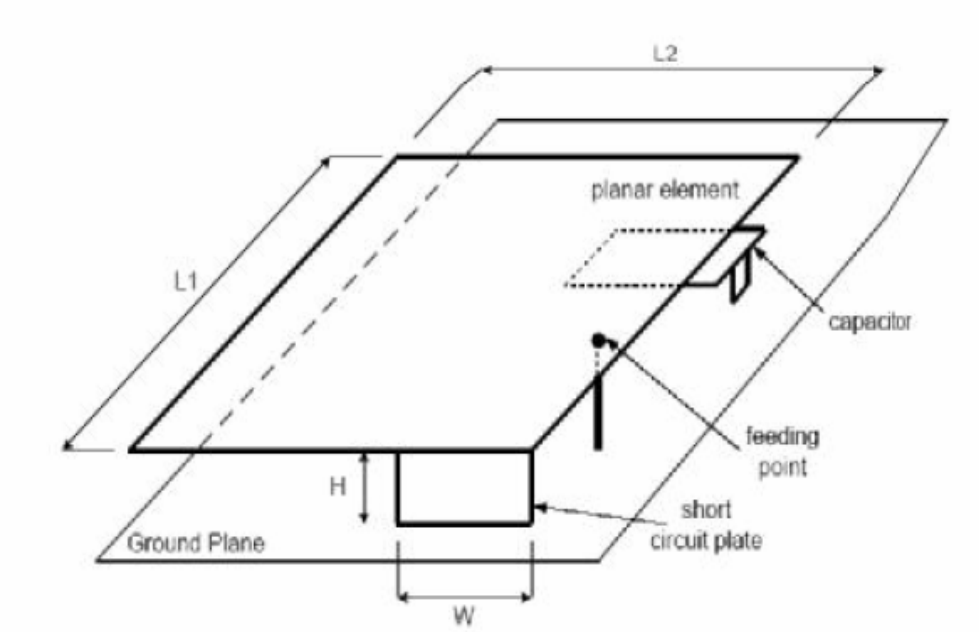

Figure 2.13: Geometry of the Planar Inverted-F Antenna
[1]

The PIFA presents 2 main advantages:

1. The first one is that it can be hidden into the housing of the mobile when comparable to whip/rod/helix antennas.
2. The second one is that it can reduce backward radiation toward the users head, minimizing the electromagnetic wave power absorption (Specific Absorption Rate (SAR)) and enhance antenna performance.

How to increase the bandwidth for PIFA?

First of all the size of the ground place affects the bandwidth. By varying the size of the ground plane, the bandwidth of a PIFA can be adjusted [1]. For example, reducing the ground plane can effectively broaden the bandwidth of the antenna system. The main goal is to reduce the quality factor of the structure and to increase the bandwidth. To achieve that aim several slits at the ground plane edges can be inserted:

- Using parasitic resonators with resonant lengths close to main resonant frequency.
- Excitation of multiple modes designed to be close together or far apart depending on requirements.

- Using stacked elements will increase the bandwidth [1].

PIFA dimensions

If we shorten the antenna we can reduce the size of the PIFA but this technique will affect the impedance at the antenna terminals. In practice, the missing antenna height is replaced with an equivalent circuit, which improves the impedance match and the efficiency. The capacitive loading reduces the resonance length from $\lambda/4$ to less than $\lambda/8$ at the expense of bandwidth and good matching. The capacitive load can be produced by adding a plate (parallel to the ground) to produce a parallel plate capacitor [1].

Resonant frequency

- The resonant frequency of PIFA can be approximated with [1]:

$$L1 + L2 = \lambda/4 \tag{2.17}$$

Moreover the ratio $\frac{L1}{L2}$ influences the resonant frequency: the higher this ratio the lower the resonance frequency will be. The PIFA resonance frequency is proportional to the current distribution effective length. To clarify the previous statement we will deal with simple conditions [3]:

1. If the width of the short circuit plate W equals the whole length of the planar element L1, we have a $\frac{\lambda}{4}$ antenna. So we have $\frac{W}{L1} = 1$ and the resonance frequency can be expressed as:
$$f_{r_1} = \frac{c}{4(L2 + H)} \tag{2.18}$$
with $L2 + H = \frac{\lambda}{4}$, c is the speed of light and H is the short-circuit plate height.
2. If $W = 0$, we get an infinitesimal short circuit pin:
$$f_{r_2} = \frac{c}{4(L1 + L2 + H)} \tag{2.19}$$
with $L1 + L2 + H = \frac{\lambda}{4}$.
3. If $0 < W < L1$,
$$f_{r_2} = \frac{c}{4(L1 + L2 + H - W)} \tag{2.20}$$
4. When $0 < \frac{W}{L1} < 1$, we can approximate the resonance frequency with a linear interpolation operation:
$$f_r = \frac{W}{L1} f_{r_1} + (1 - (\frac{W}{L1})^{\frac{L1}{L2}}) \tag{2.21}$$

- The introduction of an open slot reduces the frequency. This is due to the fact that there are currents flowing at the edge of the shaped slot, therefore a capacitive loaded slot reduces the frequency and thus the antenna dimensions drastically. The same principle of making slots in the planar element can be applied for dual-frequency operation as well.

- The width of the short circuit plate of the PIFA plays a very important role in governing its resonant frequency. Resonant frequency decreases with the decrease in short circuit plate width, W.
- Unlike micro-strip antennas that are conventionally made of half wavelength dimensions, PIFAs are made of just quarter-wavelength.
- By analyzing the resonant frequency and the bandwidth characteristics of the antenna we can easily determine the site of the feed point, in order to obtain the minimum reflection coefficient.

Impedance matching

The impedance matching of the PIFA is obtained by positioning of the single feed and the shorting pin within the shaped slot, and by optimizing the space between feed and shorting pins [1].

Radiation pattern

- The radiation pattern of the PIFA is the relative distribution of radiated power as a function of direction in space.
- In the usual case the radiation pattern is determined in the far-field region and is represented as a function of directional coordinates. Radiation properties include power flux density, field strength, phase, and polarization.

Electric field distribution

The dominant component of the electric field Ez is equal to zero at the short-circuit plate while the intensity of this field at the opposite edge of the planar element is significantly large. For fields Ex and Ey there is pointy part, which corresponds to the feed source. It means that the electric line of force is directed from feed source to the ground plane. Then, when the width of the short-circuit plate is narrower than the planar element, the electric field Ex and Ey start generating at all open-circuit edges of the planar element [1].

Current distribution

PIFA has very large current flows on the undersurface of the planar element and the ground plane compared to the field on the upper surface of the element. Due to this behavior PIFA is one of the best candidate when we talk about the influence of the external objects that affect the antenna characteristics (e.g. mobile operators hand/head). PIFA surface current distribution varies for different widths of short-circuit plates. The maximum current distribution is close to the short pin and decreases away from it [1].

Efficiency

The efficiency of PIFA in its environment is reduced by all losses suffered by it, including: ohmic losses, mismatch losses, feedline transmission losses, edge power losses, external parasitic resonances.

2.4 FDTD

FDTD is a popular computational electrodynamics modeling technique. It is a time-domain method so the solutions can cover a wide frequency range with a single simulation run. This method works modifying Maxwell's equations in differential form to central difference equations, that can be solved easily in software. Maxwell's equations (in partial differential form) are modified to central-difference equations, discretized, and implemented in software. The equations are solved in a progressive way: the electric field is solved at a given instant in time, then the magnetic field is solved at the next instant in time, and the process is repeated over and over again [18]. As every field of engineering, the widespread of the FDTD traces back its origins to military applications, such as the reduction of the radar cross-section of airplanes and missiles [19].

Since 1990, FDTD techniques have emerged as primary means to computationally model many scientific and engineering problems dealing with electromagnetic wave interactions with material structures. Current FDTD modeling applications range from near-DC (ultralow-frequency geophysics involving the entire Earth-ionosphere waveguide) through microwaves (radar signature technology, antennas, wireless communications devices, digital interconnects, biomedical imaging/treatment) to visible light. Because of the dependence between the electric and magnetic fields, Yee developed an algorithm to solve both electric and magnetic fields in space and time using the aforementioned Maxwells equations, which form is coupled and interlinked. In order to use the FDTD algorithm, it is necessary to specify a computational domain, describing properly all the geometrical objects inside the domain. These objects are made up by specific materials and we can specify the properties of these materials such as:

- The Geometry of the entities
- The Free-space properties, such as the free space permittivity and permeability
- Some other FDTD parameters such as the cell size, the time step, the frequency resolution in the Fast Fourier Transform (FFT) spectra and the maximum number of time steps
- The Domain boundaries

Thanks to FDTD, complex three-dimensional systems can be modeled and analyzed, including microwave interaction with human body or non-linear components simulation. The structure under analysis can be made up by constitutive materials with special features, such as lossy dielectrics, anisotropic media or magnetized ferrites.

Because of the possibility of using the so called near to far transformations, the antenna far field pattern can be obtained, together with the derivation of currents and power flows. The input impedance of the antenna can be calculated thanks to a broadband simulation, in order to study both impedance matching and antenna efficiency. It is interesting to remember that we can also display real-time animations, that contributes to a deeper understanding of the physical behavior of the structure under simulation [2].

2.4.1 Time step parameter

One important parameter in the FDTD simulation is the time step parameter. Simulations can require many thousands of time steps for completion. Depending on the number of time

steps we mention for a simulation, we can get different results: their main difference will be their accuracy. The more we add time steps for a simulation, the more we will get accuracy in the geometry of the curve. It is possible to verify using for a same antenna, different time steps simulations. In our case, we did only one simulation and then we have been able to get the results if we had used less time steps. This required to make two FFTs on:

- the truncated output voltage
- the truncated source voltage

We truncated these voltages to the number of desired time steps (which is inferior to the initial size). The figure 2.14 shows three curves that we got for a same simulation but with different number of time steps.

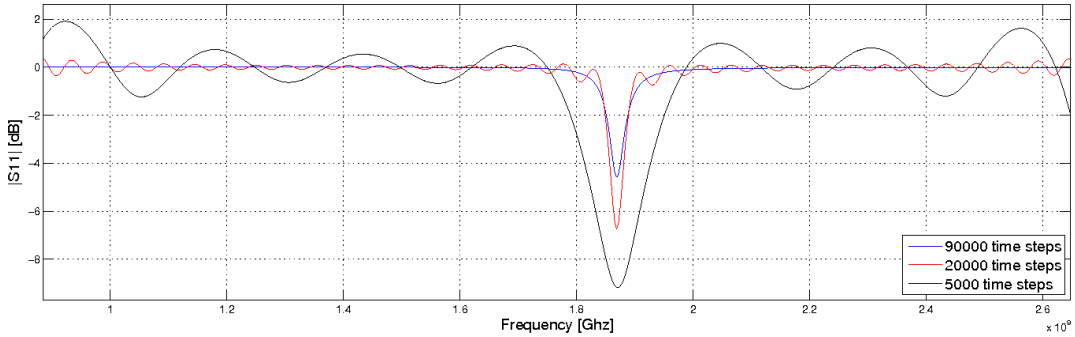

Figure 2.14: Comparison based on the number of time steps

The black curve is the one which has the less number of time steps (5000 time steps). The blue one is the curve that has the more number of time steps (90000) and the best precision. The red curve has 20000 time steps. The center frequency stays the same independently of the number of time steps. But we can notice something important for the S_{11} parameter: when the number of time steps is not sufficient, the curves reach values superior to zero for the reflection coefficient which is an error. Indeed we have a passive antenna thus a positive value for the reflection coefficient is not correct. The more we put time steps for a simulation, the less errors we get with the curve we obtain. Furthermore, we can notice how much the bandwidth becomes narrow with less time steps. The results obtained with a low number of time steps will be very optimistic compared to the reality concerning the bandwidth. In order to avoid long computation time and have better results with a minimum number of time steps, it is possible to use an estimation algorithm using the Forward-Backward Autoregressive (AR) Model[29].

Forward-Backward AR Model

We used Matlab software in order to estimate and predict the shape of the signal based on simulated time steps. If a discrete time series x(1), x(2),..., x(p) is to be modeled as in the equation 2.22, we calculate the Forward-Backward AR a_1, a_2,...,a_n parameters. Figure 2.15 shows the time domain results .Figure 2.16 shows the S11 results in frequency domain we had using the 50^{th} order Forward-Backward AR Model. In this simulation we used as a basis 15000 FDTD simulated time steps (the blue curve). The goal is to obtain results for

40000 time steps (the red curve) so estimating 25000 time steps. The third curve shows the results if we had simulated with FDTD for 40000 time steps. We can notice that the model doesn't totally match with the FDTD but at least it is more realistic than without estimation. Another thing we have noticed during our investigation and that confirms the theory, is that the higher is the order, the better are the results. The figure 2.17 shows clearly how better becomes the reflection coefficient when increasing the order. However, we can still notice that there is a difference between what the FDTD simulate and our approximation. That is caused by the model that is not accurate enough. We haven't investigated other type of model as it is not the main goal of our project. But this could be done in a future work in order to have much better results compared to the one we had.

$$x(n) = -a_1 x(n-1) - a_2 x(n-2) - ... - a_p x(n-p) + q(n) \tag{2.22}$$

where x_j is the signal value at step j and $q(n)$ is a white noise process whose variance also has to be found to carry out the extrapolation of the signal [29].

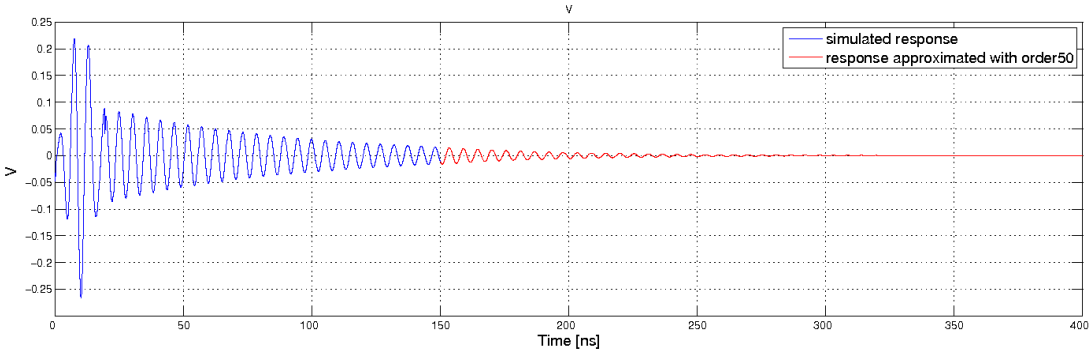

Figure 2.15: Time domain estimation

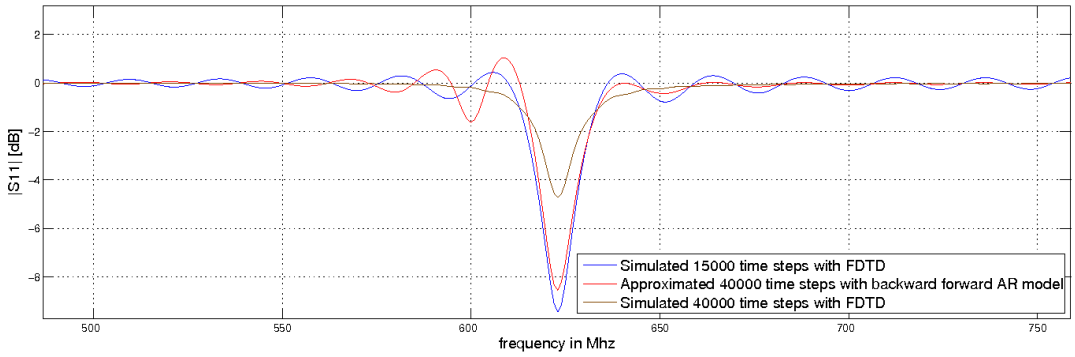

Figure 2.16: Improvements using the AR estimation

2.5 Switching circuits

One of the main goals in designing a DVB-H antenna is to achieve the required bandwidth for DVB-H with an embedded antenna. When an antenna doesn't cover the whole needed

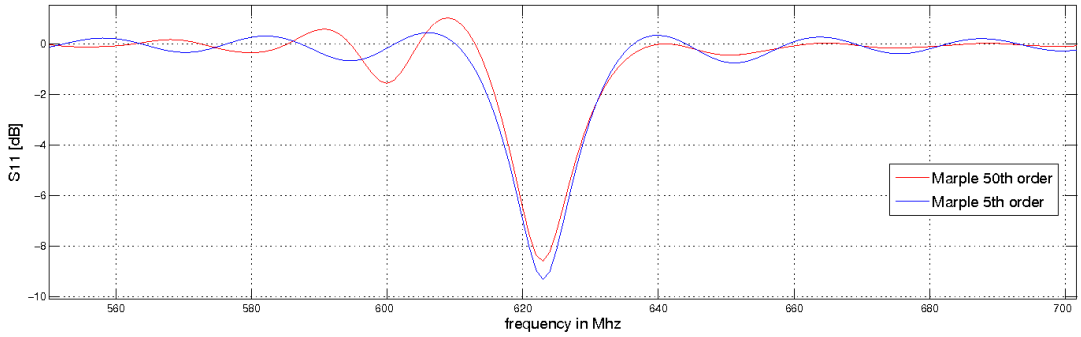

Figure 2.17: Improvement of the estimation using higher order

bandwidth, it is possible to tune it using switching circuits. A switching circuit should be considered as an interruptor: it means that it can have two or more different states and is used to make the link between two elements or more elements of a circuit.

The switching circuits could be placed in two different places:

- Depending on the frequency band we want to use, we will have to choose between different impedance matching circuits. The impedance matching circuit enables us to tune the antenna to a desired frequency. It is possible to put before them a switching circuit that will choose which one to use. Figure 2.18 describes its principle.
- Another solution to tune the antenna in different band, would be to put the switching circuit directly on the antenna. So that we could vary the electric size of the antenna and then have different frequencies covered. Figure 2.19 describes its principle.

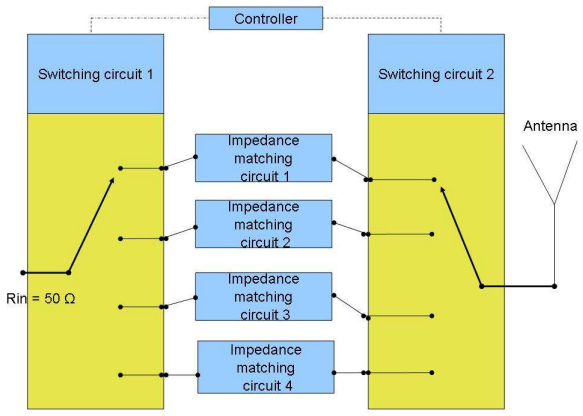

Figure 2.18: Switching on different matching circuits

In order to implement switching circuit, it is possible to use many different components. Positive intrinsic negative (PIN) diodes are very often used in telecommunications as switches for their high switching speeds, commercial availability, low cost, and ruggedness.

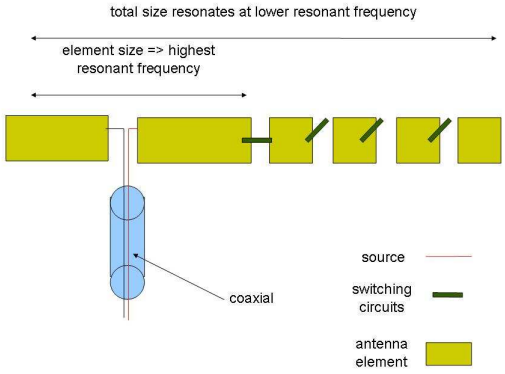

Figure 2.19: Modifying the antenna size with switch

The progress made on Micro-Electro-Mechanical Systems (MEMS) let us think that they would be well used as switches with low insertion loss, high isolation and linearity, low power consumption and mass, long lifetime. The main problem with MEMS is that they are very difficult to get as the industry is not ready for their mass fabrication.

It is also possible to use reed relays. A reed relay consists of a coil wrapped around a reed switch. The switch is composed of two overlapping ferromagnetic blades (called reeds) that are hermetically sealed within an inert-gas-filled glass capsule. When current flows through the coil, a magnetic field is produced that pulls the two reeds together. This completes a signal path through the relay. When the coil is de-energized, the spring force in the reeds pulls the contacts apart. Figure 2.20 and figure 2.21 show respectively an open reed relay and a closed reed relay [32].

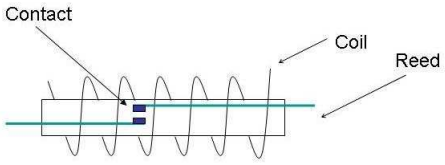

Figure 2.20: Open Reed Relay

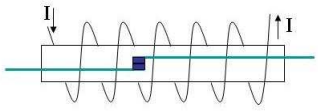

Figure 2.21: Closed Reed relay

Reed relays have several advantages such as their small size and the good bandwidth and the good isolation they provide [32].

The table 2.3 makes a comparison between MEMS, PIN diodes and Reed relay parameters.

Table 2.3: Performance comparison of PIN Diode and RF MEMS Electrostatic Switches [20]

Parameter	RF MEMS	PIN DIODES	REED RELAY
Voltage (V)	20 - 80	$\pm$3 - 5	5
Current (mA)	0	0 - 20	50
Power Consumption (mW)	0,5 - 1	5 - 100	167
Switching	1 - 300μs	1 - 100 ns	100 μs - 300 μs
Loss (1 - 100 GHz) (dB)	0.1 - 0.4	0.3 - 1.2	< 1

Chapter 3

Preliminary study

In the researches we made we have been able to find three master thesis which topic was DVB-H antenna. The first one was done by Jari Holopainen [7] at the department of Electrical and Communications Engineering of Helsinki university in 2005. The second one was made at Lund university by Fredrik Persson and Mattias Wideheim [6] in Junuary 2006. The last one was made at Aalborg University by Mauro Pelosi [4] in June 2006. We will use these documents as a starting point and improve the work that has been done. In the following paragraphs, we will make a description of the work done using the best antennas they designed. After that we will show how to improve these antennas.

The investigated antennas are the following:

1. Fredrik and Mattias's loop antenna
2. Pifa and pifa with lumped element
3. Mauro's antenna
4. Jari's antenna

3.1 Fredrik and Mattias's loop antenna

The antenna studied here did not lead to promising results. Indeed the antenna size was too big . The detailed results are presented in appendix G where we explained why this antenna cannot be chosen for DVB-H reception in a small device.

3.2 PIFA and PIFA with lumped element

It has been investigated in Mauro Pelosi's master thesis [4] that the more the ratio between the not short circuit length and the short circuit length of the PIFA is large, the more the quality factor of the antenna decreases. Adding an offset towards the feeding point will increase the resonance frequency and decrease the quality factor. Increasing the height of the short circuit plate decreases even more the quality factor.

The use of lumped components between the antenna and chassis as shown in figure 3.1 enables us to tune the antenna. Increasing the capacity of the lumped component will decrease the resonance frequency of the antenna and the impedance bandwidth but also increase the

values of the quality factor and the real part of the input impedance. The problem using the lumped elements is that the capacitors' values are very small (1 pF) for our band of frequency and so they are influenced by the surrounding environment. The parasitic effect appears at high frequency when the components cannot be characterized by their "ideal" response. Added to this, they increase the power loss due to their insertion.

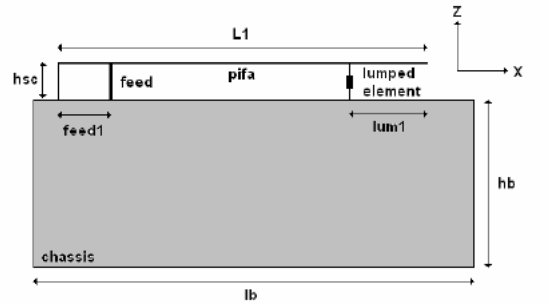

Figure 3.1: Lumped Pifa
[4]

3.3 Mauro's antenna:

The best antenna we found in Mauro's thesis, is the top meandered antenna shown in figures 3.2, 3.3, 3.4.

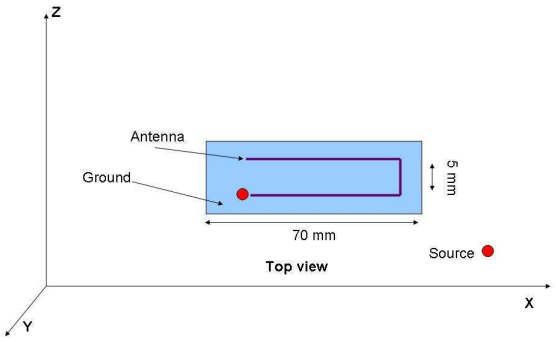

Figure 3.2: Meandered Monopole - Top view

In figure 3.5 are shown the results that Mauro obtained for a matching level at 0.7 (i.e.$-3dB$) and figure 3.6 shows our own results using exactly the same antenna than Mauro. We can notice that he used only 7 matching circuits whereas we used 10. The difference may be due to to the fact that we did not use the same FDTD simulator. Our results look more realistic as they show clearly how the bandwidth becomes more and more narrow when going to lower frequencies.

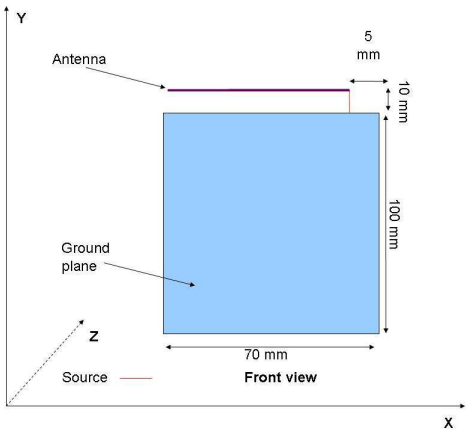

Figure 3.3: Meandered Monopole - Front view

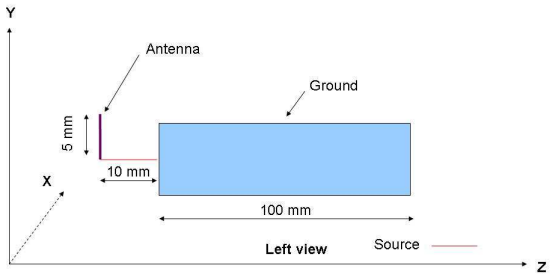

Figure 3.4: Meandered Monopole - Left view

Then we simulated the same antenna for a matching level at 0.5 (i.e.$-6dB$). The results are shown in figure 3.7: we covered the whole band using this time 18 matching circuits. We notice that the more we go down in frequency, the more the bandwidth becomes narrow. This antenna ends up with a frequency band of 6 Mhz at 470 Mhz which is inferior to one DVB-H channel bandwidth which is 8 Mhz. Furthermore when we look at the corresponding Q factor, we can see that it is quite high (more than 100). The good point with this antenna is its size (3,25 cm^3).

3.3.1 L-matching network solution

For Mauro's antenna, we are going to explain how we did to get the matching circuits on the graph. Depending on the matching level that we want we adjusted the resonance frequency of the circuit in order that we get the intersection of the matching level and the frequency limits. In order to match the antenna impedance, we have used the L-matching circuit. From the

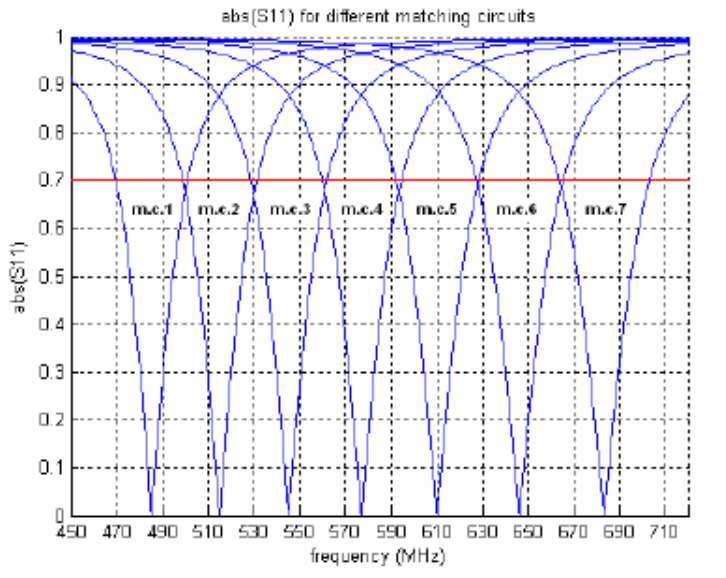

Figure 3.5: Top meandered antenna - S11 parameter using matching circuits - Mauro's results at -3 dB

[4]

formulas in appendix D, we can calculate the values of the admittance B and the impedance X. These values determine lumped components' values. Figures D.1 and D.2 present the circuit design. If B is positive then the component is considered as a coil. Then L = $2\pi f_0 B$ where f_0 is the matching frequency. The impedance Z_b is:

$$Z_b = j\omega L \tag{3.1}$$

If B is negative then the component is considered as a capacitor. Then C = $\frac{-B}{2\pi f_0}$. The impedance Z_b is:

$$Z_b = \frac{1}{j\omega C} \tag{3.2}$$

If X is positive then the component is considered as a coil. Then L = $\frac{2\pi f_0}{X}$ where f_0 is the matching frequency. The impedance Z_x is:

$$Z_x = j\omega L \tag{3.3}$$

If X is negative than the component is considered as a capacitor. Then C = $\frac{-1}{2X\pi f_0}$. The impedance Z_x is:

$$Z_x = \frac{1}{j\omega C} \tag{3.4}$$

where $\omega = 2\pi f$.

Depending on the case we are $real\{Z_a\} \geq Z_0$ or $real\{Z_a\} \leq Z_0$, we have two different L-matching circuits (Z_a is the impedance of the antenna and Z_0 the impedance to be matched). Once the matching circuit lumped elements' impedance have been found, we calculate the total impedance Z_T. This total impedance is frequency dependant as the antenna impedance

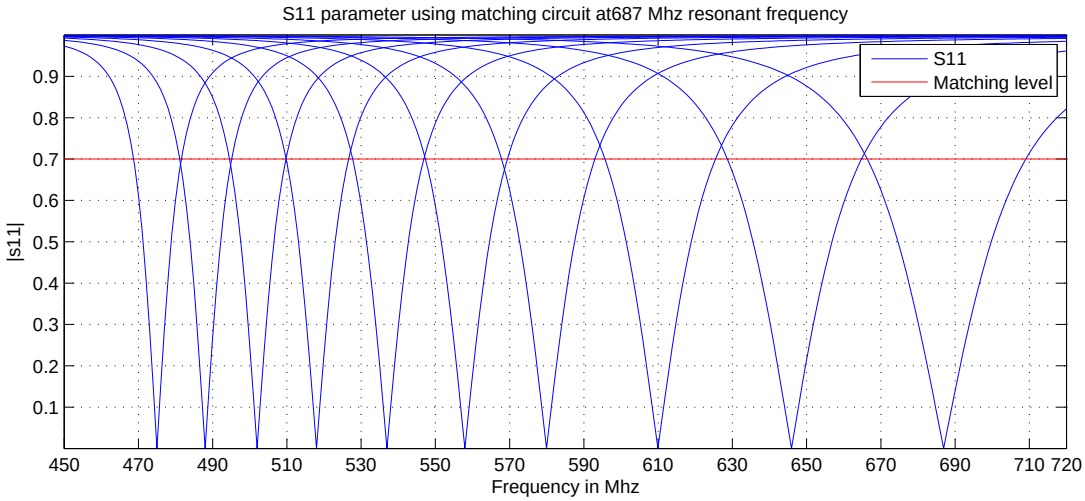

Figure 3.6: Top meandered antenna - S11 parameter using matching circuits - Our results at -3 dB

Z_a and the matching circuit impedance are both frequency dependant. If $real\{Z_a\} \geq Z_0$, the total impedance Z_T will be :

$$Z_T = Z_x + \frac{1}{\frac{1}{Z_b} + \frac{1}{Z_a}} \tag{3.5}$$

Otherwise $real\{Z_a\} \leq Z_0$ will give an impedance matching Z_T:

$$Z_T = \frac{1}{\frac{1}{Z_b} + \frac{1}{Z_a + Z_x}} \tag{3.6}$$

Finally, we calculate the reflection coefficient S_{11}:

$$S_{11} = \frac{Z_T - Z_0}{Z_T + Z_0} \tag{3.7}$$

3.4 Jari's antenna

Another very interesting antenna we found is the one made by Jari Holopainen shown in figures 3.8, 3.9, 3.10.

This antenna also uses impedance matching circuits in order to cover the whole bandwidth: it has a dual-resonant matching circuit. In his matching circuit, Jari used a serie inductance which value is 2,7 ηH, a parallel inductance which value is 8,2 ηH and a parallel capacitance which value is 12 pF. He obtained a double resonator.

We tried to simulate the same antenna as Jari using the same values for the components of the matching circuits. We did not obtain a double resonator.

We simulated again his prototype but changing the values of the components of the matching circuit in order to try to get a double resonator. On figure 3.12, one curve is the one we got using Jari's components values (blue curve) and the other curve is the one we got changing the values of the components of the matching circuit, trying to get a double resonator. We

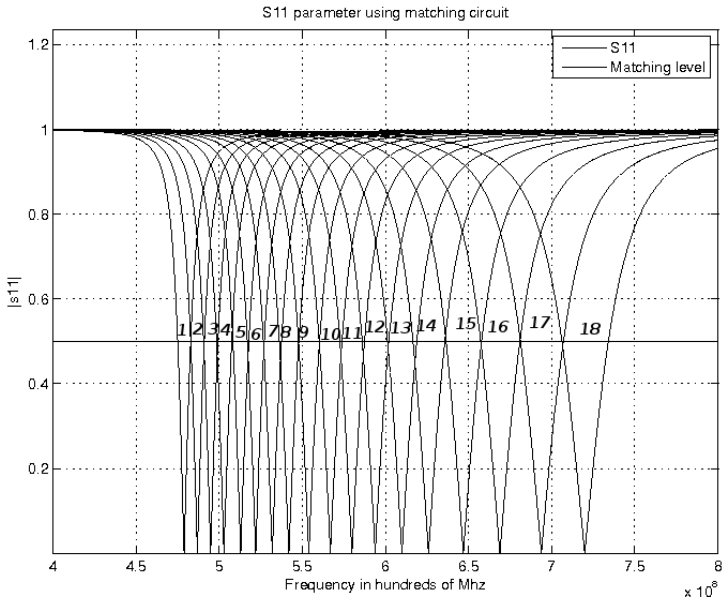

Figure 3.7: Top meandered antenna - S_{11} parameter using matching circuits - Our results at -6 dB

got a double resonator with the new values (red curve in figure 3.12). However the matching level was too low: inferior to -0.5 dB. Furthermore the antenna size is $9.75cm^3$ which is 3 times superior to the maximum size available in our case.

Table 3.1: Quality factor and bandwidth of Mauro's antenna's band

Band number	Bandwidth (Mhz)	Q
1	6	118
2	8	121
3	8	124
4	8	126
5	8	133
6	9	139
7	10	148
8	10	167
9	12	197
10	13	216
11	14	224
12	15	227
13	16	287
14	18	770
15	20	968
16	23	187
17	25	273
18	27	863

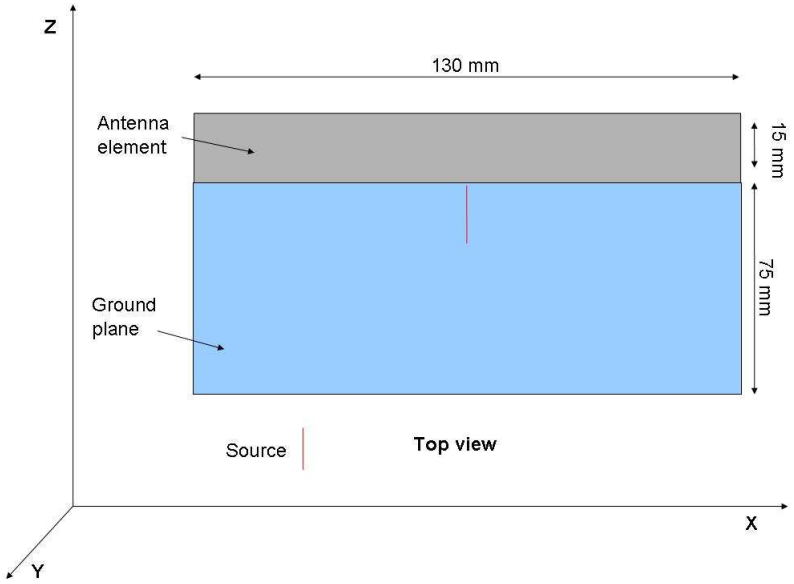

Figure 3.8: Jari's antenna - Top view

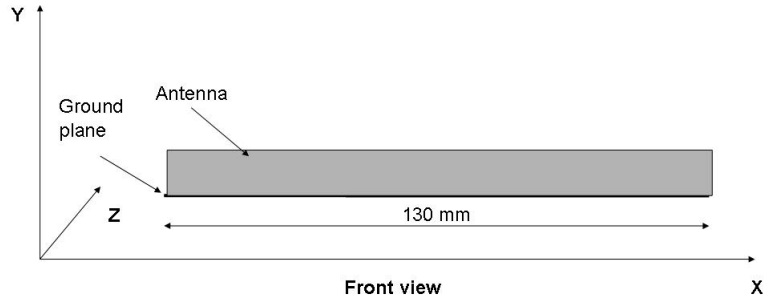

Figure 3.9: Jari's antenna - Front view

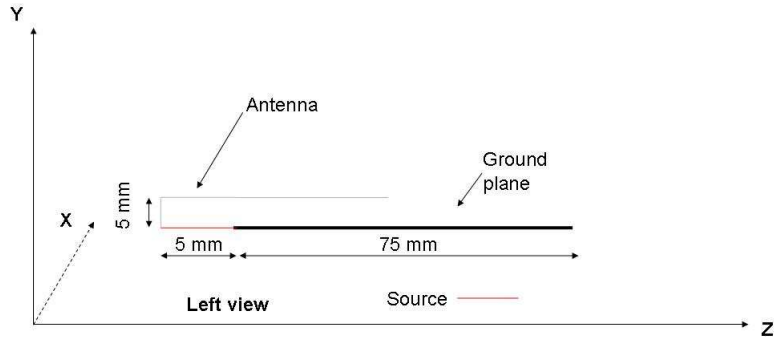

Figure 3.10: Jari's antenna - Left view

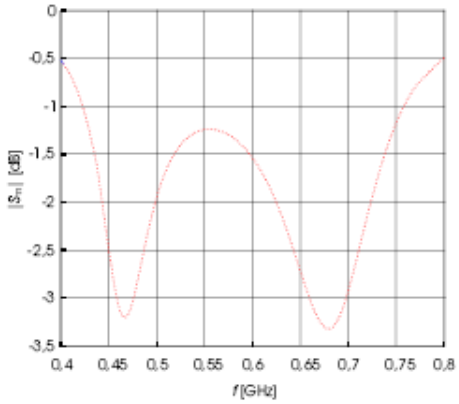

Figure 3.11: Jari's antenna - S_{11} parameter using matching circuits - Jari's results [7]

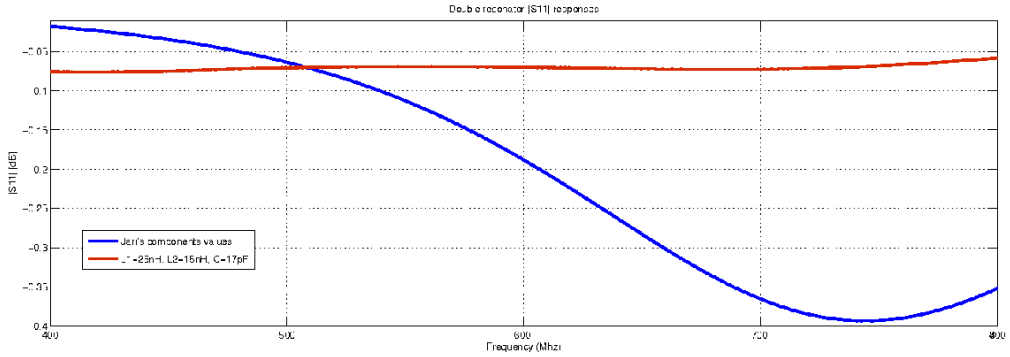

Figure 3.12: Our results using Jari's antenna: the blue curve is with his components value and the red one is with our components value (L1=25nH - L2=15nH - C=17pF)

Chapter 4

Analysis and improvements

As seen in the previous chapter, the use of matching circuits is necessary if we want to be able to cover the whole DVB-H band with a small antenna. The main problem is that using simple matching circuits will lead to the superposition of much more than one matching circuit and then it will increase the losses. The goal here is to improve the performances of the receiver using broadband matching techniques. Using the work done in the section "Preliminary study", we finally decided to focus on Mauro's antenna because we did not get the same results as Jari while working on his antenna. Moreover Mauro's antenna is easy to build as it looks like a wire and its size is $3.25cm^3$ which fits with our assuption's size. The results we got for Mauro's antenna led us to the choice of 10 matching circuits to cover the whole DVB-H band which may increase the losses in our design. We decided to implement a Chebyshev bandpass impedance matching network in order to improve considerably the bandwidth. This has been done according to appendix H which describes how the bandpass impedance matching networks are designed.

First of all we will see in this chapter the results obtained by the implementation of our bandpass impedance matching network following appendix H. The results will be presented using Mauro's antenna. Then we will calculate the return losses of the matching circuits and the insertion losses of the switches.

4.1 Chebyshev bandpass impedance matching network

Chebyshev response type has been chosen instead of Butterworth and maximally flat responses because it provides the fastest slope compared to the others (the transition region is the narrower). Furthermore, the presence of the ripple in the Chebyshev response doesn't affect us as long as it stays below our matching limit. The theory says that the more we want a good degree of impedance match for one frequency band, the more the ripple has to be large. The smaller the ripple, the worst the degree of matching is. The figure 4.1 shows the S_{11} Chebyshev response for a constant antenna impedance over the whole band. This figure confirms the theory: the blue curve shows a matching degree at -16 dB at the price of a large ripple of 9.5 dB while the red curve shows a smaller ripple of 1.5 dB at the price of a worst matching degree. This figure also confirms Fano's law that says that a good matching level cannot be done over the whole bandwidth. As it can be seen, the red curve covers a larger bandwidth than the blue curve but with a lower matching level.

4.1.1 Impact of the L_{Ar} and L_r parameters on the reflection coefficient

In order to better understand the effects of the different parameters involved in the design of the Chebyshev matching circuit, we have plotted different results according to their variation. The figure 4.2 shows how the L_r parameter defined in appendix H affects the S_{11} coefficient. When increasing this parameter, it will decrease the matching. This parameter is mainly used to balance the matching of the double resonance. It appears that decreasing it will suppress one of the resonance but improve the matching level. However because the serie capacitors' value of the matching network is directly linked to the L_r's value as shown in equation H.25, L_r shouldn't be too small. In that case it would lead to high capacitor component's value.

The figure 4.3 shows how the maximum ripple attenuation loss (L_{Ar}) parameter affects the S_{11} coefficient. Increasing its values will increase the mismatch. It appears that the value of L_{Ar} has to be searched in function of L_r in order to increase considerably the bandwidth. The figure 4.4 shows how should the matching circuit look like in order to have the double resonance.

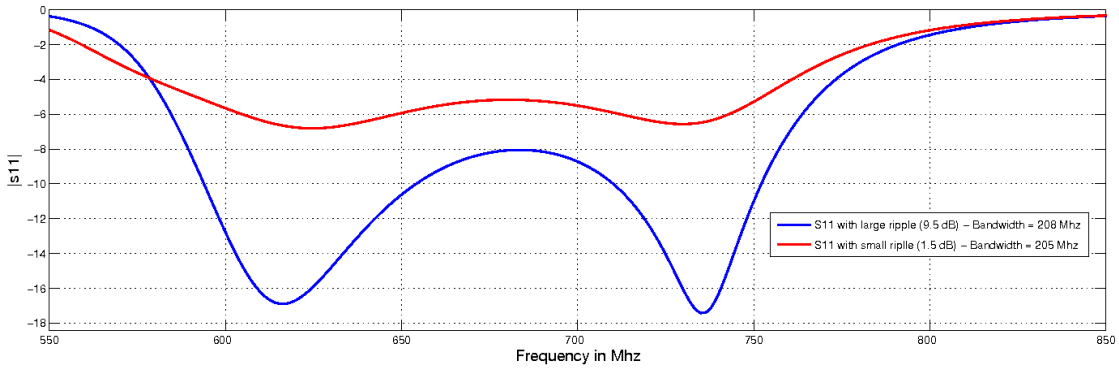

Figure 4.1: Ripple size VS reflection coefficient

4.1.2 Mauro's antenna with a Chebyshev matching circuit

In this section we are going to explain how we designed the second order matching circuit for Mauro's antenna. We will follow the steps described in appendix H. Figure 4.5 shows the impedance while figure 4.6 shows the admittance of Mauro's antenna. It is seen that the real part of the impedance is more constant than the real part of the admittance. The antenna can then be presented as a RLC series resonator. In order to bring it to resonance at f_0, we will put a serie reactance. If the imaginary part of the antenna at f_0 is positive, a capacitor is used to bring it to resonance with

$$C = \frac{1}{w_0 imag(Z_a(f_0))}$$

If the imaginary part of the antenna at f_0 is negative, a coil is used to bring it to resonance with

$$L = \frac{-imag(Z_a(f_0))}{w_0}$$

where $Z_a(f_0)$ is the impedance of the antenna at frequency f_0.

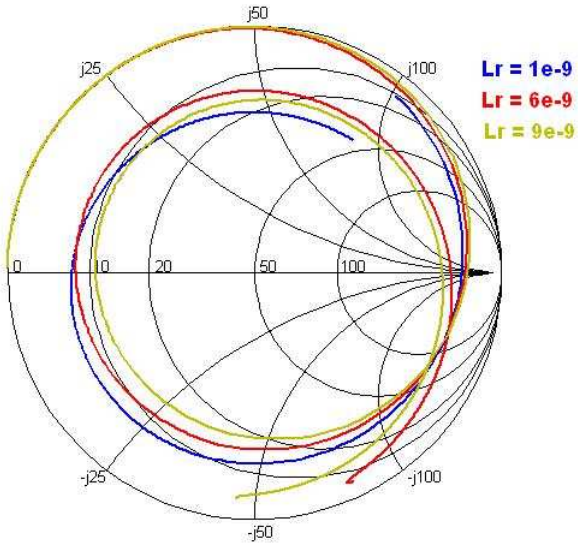

Figure 4.2: Reflection coefficient in function of L_r

Then we calculated the low pass prototype parameters according to appendix H. The figure 4.7 shows that we are able to cover the whole DVB-H band using only 5 matching circuits. The table 4.1 gives the values for each matching circuits we used in order to cover the whole band. The figure 4.8 presents the topology of our circuit.

4.1.3 End to end loss

The end to end loss of our whole design has to take into consideration the following parameters:

- The losses due to the antenna (its characteristics such as its material)
- the losses due to the reflection, called reflection loss : $L_{refl} = 10 \log \frac{1}{1-|\rho|^2}$
- the insertion losses
- the losses due to the switches

The figure 4.9 presents the reflection losses of the antenna for ideal components using chebyshev matching circuits while figure 4.10 presents these using L-matching circuits. Because we are using half the number of matching circuits with Chebyshev, we will have to use 2 switches of 5 gates while in Mauro's design 4 switches were necessary. Furthermore, when using L-matching circuits, the covered bandwidth for the lowband was inferior to one DVB-H channel. The use of our matching circuit will decrease the total insertion loss due to the switching elements. This is why it is important to well choose the type of switch. As we were not able to obtain MEMS, our choice was limited to PIN diodes and Reed relays. We have chosen 0.7 dB as a switch insertion loss. Figure 4.11 presents the losses using our matching circuit taking into account the switches' losses while figure 4.12 presents those generated by the L-matching circuits. We can see an improvement of 1.5 dB. It would be useful to include the matching circuit insertion losses and the antenna losses to have the end to end losses

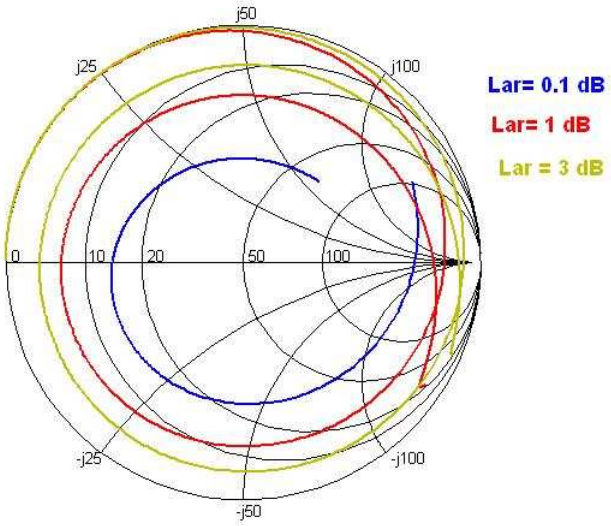

Figure 4.3: Reflection coefficient in function of L_{Ar}

of our system. As it can be seen we are fulfilling the DVB-H requirements for designing an antenna.

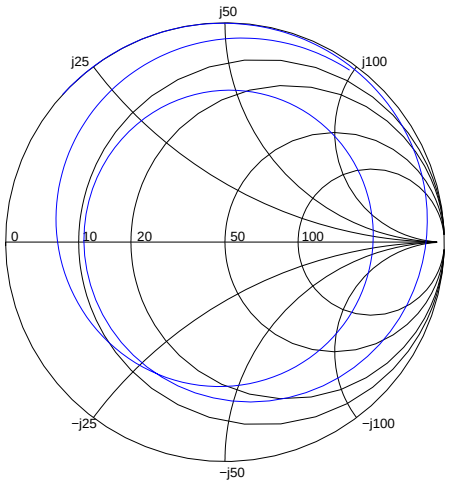

Figure 4.4: Smith Chart of a double resonant matching circuit

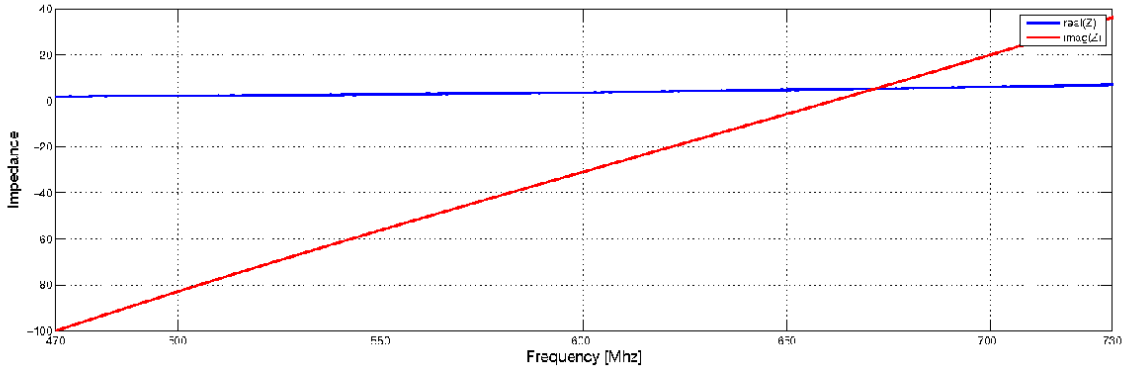

Figure 4.5: Impedance of Mauro's antenna

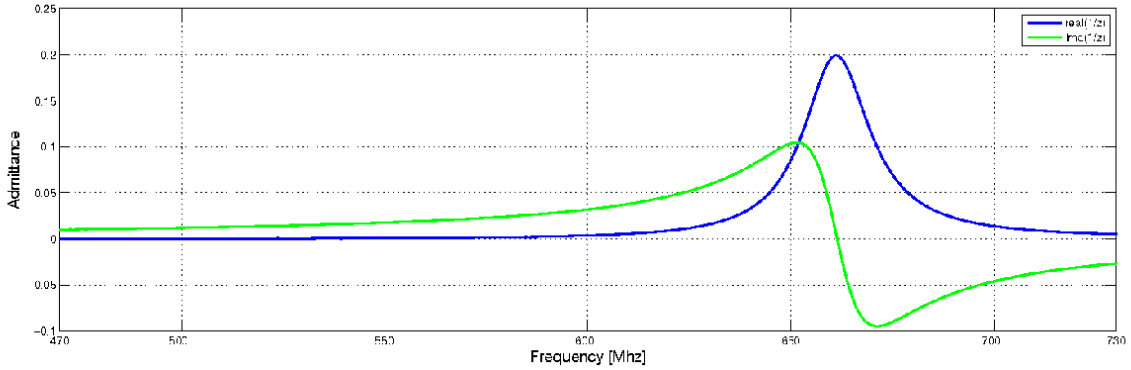

Figure 4.6: Admittance of Mauro's antenna

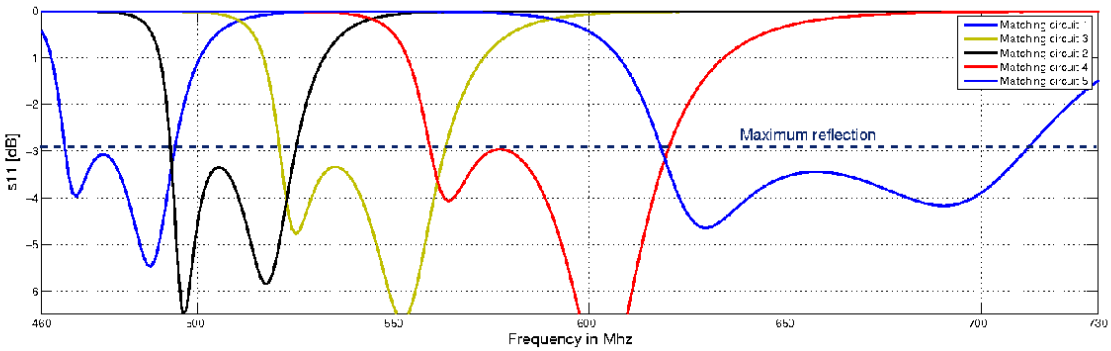

Figure 4.7: S_{11} parameter using Chebyshev impedance matching network

Table 4.1: Matching circuits characteristics

Matching circuit	1	2	3	4	5
Bandwidth [Mhz] at -3dB	28	32	42	61	100
Band edges [Mhz] at -3dB	466 - 494	494-525	522 - 562	560 - 621	620 - 720
Series reactance	28.02 nH	21.42 nH	14.50 nH	6.16nH	8.30 pF
C_1[pF]	34.72	31.37	26.03	20.35	7.124
C_2[pF]	34.72	31.37	26.03	20.35	7.124
L_0[nH]	23.34	23.10	23.21	23.12	46.25
L_1[nH]	22.13	22.08	21.78	21.34	36.49
L_2[nH]	1.31	3.79	1.50	0.12	2.27
L_3[nH]	3.12	5.40	3.66	2.94	0.03
M_{01}[nH]	6.66	6.40	7.79	9.88	23.75
M_{12}[nH]	2.62	2.32	3.25	4.49	17.49
M_{23}[nH]	26.88	24.10	27.34	30.06	69.97
L_r parameter	3	2.95	3.1	3.3	7
L_{ar} parameter	6	5.3	4.9	4	7.4
f_1 parameter [Mhz]	486	510	541	585	662
f_2 parameter [Mhz]	506	536	579	642	760

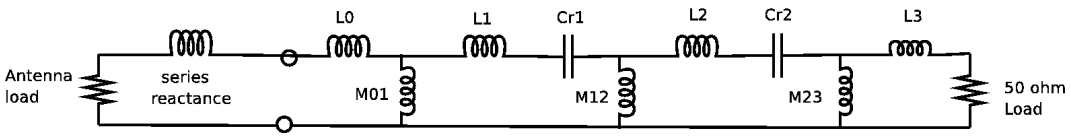

Figure 4.8: Second order Chebyshev impedance matching circuit

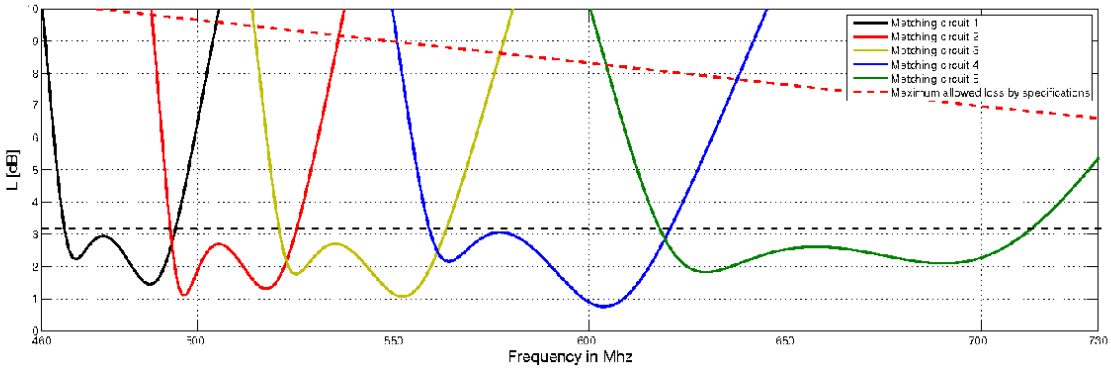

Figure 4.9: Reflection losses of Mauro's antenna using the Chebyshev matching circuit

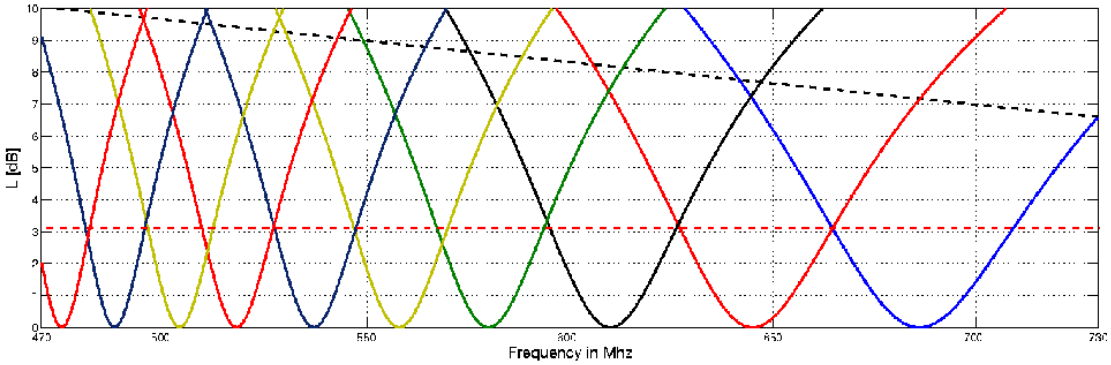

Figure 4.10: Reflection losses of Mauro's antenna using the L-matching circuit

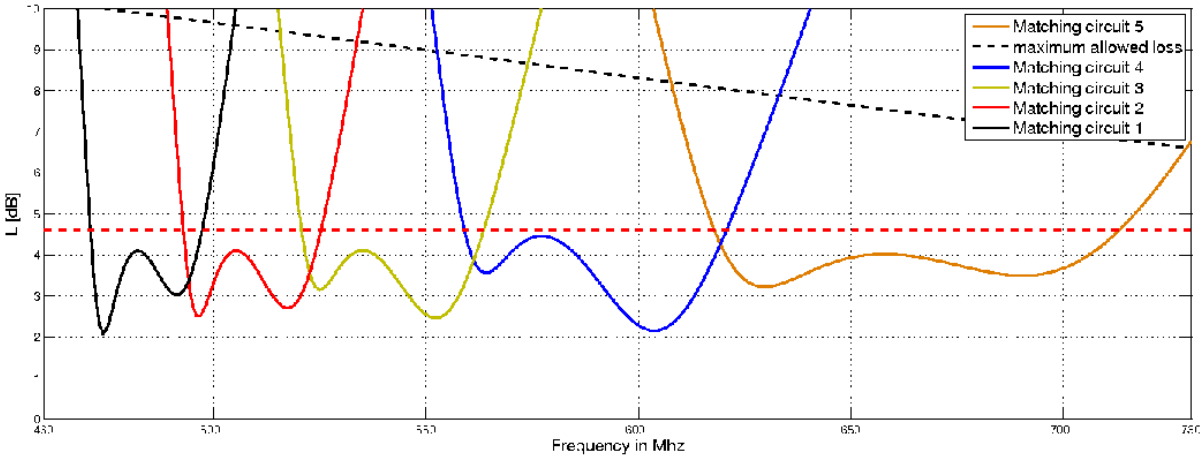

Figure 4.11: Losses of the reflexion coefficient and of the switches using the Chebyshev matching circuit

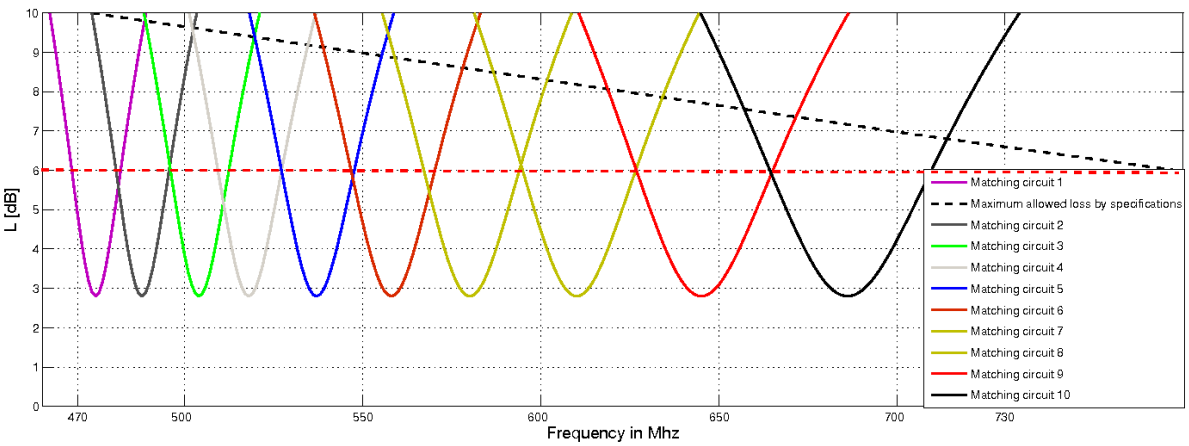

Figure 4.12: Losses of the reflexion coefficient and of the switches using the L-matching circuit

Chapter 5

Phone position

In order to find a suitable location for the DVB-H antenna, we investigated the mobile position held by users watching TV on it. The phone we used is a QTEK S200 with the following characteristics:

- The phone dimensions are 59.3*108.8*18.4 mm^3
- The screen size is 320x240 pixels
- The weight is 120g

The antenna has to be placed in a way to limit all kind of absorptions and losses.

5.1 Phone held less than 1 minute

There exist many ways to hold a mobile phone while watching television on it. Depending on how long the user will hold the phone, the way to hold it will vary from one user to another. In this section we studied the way the phone is held in a quite short time (less than one minute) with 2 users.

5.1.1 User A

User A got 2 ways to hold the phone:

1. First way: the phone is held horizontally, a hand on each side of it.
2. Second way: the phone is held vertically, the left hand holding the left side of the phone, and the right hand holding the back of the phone.

The pictures can be seen in Appendix C.

5.1.2 User B

User B got 2 ways to hold the phone:

1. First way: the phone is held horizontally, a hand on each side of it.

2. Second way: the phone is held vertically, the left hand holding the left side of the phone, and the right hand holding the right side of the phone (contrary to user A which right hand is holding the back of the phone).

The pictures can be seen in Appendix C.

5.2 Phone held more than 1 minute till 5 minutes

On our phone we added a movie which lasted about 5 minutes. We took one user asking him to watch the movie and so to hold the phone. We did this experiment in 2 different cases:

1. The user is sitting on a bed watching the movie on the mobile phone.

2. The user is waiting at a bus stop.

The pictures and the scenario can be seen in Appendix C.

We led this experiment in order to see on a handheld device where would be the more appropriate location on a mobile phone to place our antenna: meaning reducing the absorption due to the hands position.

The placement of the antenna is important: it has to be placed so that the antenna characteristics are changed as little as possible when the user holds the terminal in different ways.

A good location for the DVB-H antenna would be on the top of the phone when holding it horizontally.

Chapter 6

Conclusion and Future works

6.1 Conclusion

In this master-thesis we designed a DVB-H antenna in order to bring broadcast services to handheld receivers. Thanks to FDTD techniques we have modeled antennas such as PIFA, meandered antennas, and monopole antennas. We have been able to study different antennas' structures and analyze their impact on the bandwidth.

We found 2 master-thesis dealing with DVB-H antenna that we used as a starting point:

- Simulating Jari's antenna did not give us promising results and the antenna size was 3 times larger than the maximum volume available in our case
- Mauro's antenna (the top meandered antenna) was more suitable than Jari's especially because of its size. In order to cover the whole band of interest, we needed to use 10 matching circuits.

The use of 10 matching circuits increases the losses in our design. We aimed to find a matching network allowing us to cover the whole band of interest while minimizing the losses. This led us to the choice of the implementation of a Chebyshev bandpass impedance matching network. It improved considerably the performances of the antenna while decreasing its losses.

6.2 Future works

Based on the findings of this thesis, there are some open directions for future work. As our antenna is at least 2 dB better than the DVB-H limit all over the band, it would be possible to decrease the size of the antenna at the price of more losses while fulfilling the requirements. Decreasing the antenna size and see how much it affects losses would be a challenging direction. Furthermore, a deeper analysis and an implementation of the available estimation models would speed up the FDTD simulations. Concerning the antenna's position, it would be a good field of study to lead an experiment with more users and scenarios. Hardware implementation of our antenna and testing it to confirm our simulations would be interesting. Finally, using a DVB-H measurements tool kit and testing the reception quality will make this project complete.

Bibliography

[1] http://www.qsl.net/va3iul

[2] Mauro Pelosi, "*Tunable DVB-H antenna in a small handhled device*" Institute of Electronic Systems - Aalborg University - June 2006 - page 18

[3] Mauro Pelosi, "*Tunable DVB-H antenna in a small handhled device*" Institute of Electronic Systems - Aalborg University - June 2006 - pages 13 to 16

[4] Mauro Pelosi, "*Tunable DVB-H antenna in a small handhled device*" Institute of Electronic Systems - Aalborg University - June 2006

[5] http://www.rohde-schwarz.com/

[6] Frederik Persson and Mattuas Wideheim, "*Design of antennas for handheld DVB-H Terminals*" Department of electroscience - Lund University - January 2006

[7] Jari Holopainen, "*Antenna for handheld DVB terminal*" Department of Electrical and Communications Engineering- Helsinki University of technology - May 2005

[8] http://www.ansoft.com/converge/

[9] K. Fujimoto, A. Henderson, K. Hirasawa and J. R. James, "*Small Antennas*", ISBN: 0863800483, 1988

[10] R.C. Hansen, "*Fundamental Limitations in Antennas Proc. IEEE*", vol. 69, Feb. 1981, pages 170 to 182

[11] ETSI TR 102 377 - V1.2.1(2005-11)

[12] ETSI EN 301 192: "*Digital Video Broadcasting (DVB) and DVB specification for broadcasting*"

[13] A. Lehto, Radiotekniikka (Radio engineering, in Finnish), Helsinki, 2001, Otatieto, page 280

[14] http://www.dvb-h.org/Services

[15] Gert Frolund Pedersen, "*Basic Antennas and the need for numerical techniques*" - Aalborg University

[16] A. Lehto, RF- jamikroaaltotekniikka (RF and microwave engineering, in Finnish), Helsinki, 2002, page 267

[17] Arto Hujanen, Jan Holmberg and Johan Carl-Erik Sten, "*Bandwidth limitations of impedance matched ideal dipoles*", IEEE TRANSACTIONS ON ANTENNAS AND PROPAGATION, VOL. 53, NO. 10, OCTOBER 2005

[18] http://en.wikipedia.org/wiki/Finite difference time domain method

[19] K. S. Kunz, R. J. Luebbers, "*The finite difference time domain method for electromagnetics*" CRC Press 1993

[20] FY03 NEPP TRO - RF MEMS Switches Dr. Joanne Wellman - Jet Propulsion Laboratory - NASA

[21] Rodney Vaughan and Jorgen Bach Andersen, "*Channels, propagation and antennas for mobile communications*", 2003 - ISBN: 0852960840 - page 504

[22] Rodney Vaughan and Jorgen Bach Andersen, "*Channels, propagation and antennas for mobile communications*", 2003 - ISBN: 0852960840 - page 513

[23] Guiseppe Cali, Anders Riis Jensen, Mads Lauridsen and Normando Rosas, "*FM trasnmitter based on a PC*", Poject group, December 2006

[24] Randy Bancroft, "*Fundamental Dimension Limits of Antennas*", Centurion Wireless Technologies Westminster, Colorado

[25] G. Matthaei, L. Young, E.M.T. Jones, " *Mircowave filters, impedane-matching network, and coupling, structures*", ARTECH HOUSE, INC - 1985 - ISBN: 0-89006-099-1

[26] G. Matthaei, L. Young, E.M.T. Jones, " *Mircowave filters, impedane-matching network, and coupling, structures*", ARTECH HOUSE, INC - 1985 - ISBN: 0-89006-099-1 - Page 700

[27] G. Matthaei, L. Young, E.M.T. Jones, " *Mircowave filters, impedane-matching network, and coupling, structures*", ARTECH HOUSE, INC - 1985 - ISBN: 0-89006-099-1 - Page 99

[28] G. Matthaei, L. Young, E.M.T. Jones, " *Mircowave filters, impedane-matching network, and coupling, structures*", ARTECH HOUSE, INC - 1985 - ISBN: 0-89006-099-1 - Pages 484 and 485

[29] Vikram Jandhyala, Eric Michielssen, and Raj Mittra, Fellow, "*FDTD Signal Extrapolation Using the Forward-Backward Autoregressive (AR) Model*", IEEE MICROWAVE AND GUIDED WAVE LETERS. VOL. 4, NO. 6, JUNE 1994

[30] Gert Frolund Pedersen, Mathieu Tartiere1, Mikael B. Knudsen, "*Radiation efficiency of handheld phones*", Center for Personkommunikation, Aalborg University

[31] David M. Pozar, "*Microwave engineering*", 1990 - ISBN: 0-201-50418-9 - pages 281 to 283

[32] http://zone.ni.com/devzone/cda/tut/p/id/3953

Appendix A

Trial DVB-H transmitter in NorthJutland

In order to validate our work and to test the antenna, we wanted to get some information about the transmission parameters (frequencies channel, ERP...) in NorthJutland near Aalborg, a map of the emitters and any other useful information. We sent an email to an engineer working at NordCom Interactive Company to get the information we needed. We got the following answers.

"First of all there are a lot of problems connected to a test of DVB-H in NorthJutland. Together with TV2/Denmark and Nordjyske Medier it was planned that a pilot with DVB-H combined with DVB-T had to be made. There have been different pilots but they have all been based on low power-transmitters (very small ones) and it was for a small area. So we were ready to test in the whole region (NorthJutland). The Danish IT-og Telestyrelsen has given us the channel 63 (which corresponds to the frequency 810 MHz) and was allowed to use up to 10 KW from the transmitters. Everything sounds really good until we have been negotiating first with Motorola and then with Samsung: they were both very positive and they agreed to go into the project with receivers, but there was a very big problem: they hadn't any receivers (mobile phones with DVB-H-receivers) for receiving channels at more than channel 55 or under that frequency-spectrum. After weeks or months we had a meeting with Motorola and Samsung a few days before Easter 2007. They said that it was possible to make a pilot in the middle of Jutland with transmitters placed at the location Sparkr near Viborg. Here they could have channel 49, and they were allowed to transmit with 50 KW. But our Company is based in NorthJutland and so we didn't want to go for a pilot in another region. So we gave up."

Appendix B

N77 Nokia DVB-H phone

Nokia developed a DVB-H phone which has the following dimensions:

- Volume: 92 cc
- Weight: 114 g
- Length: 111 mm
- Width: 50 mm
- Thickness (max): 18.8 mm

The screen size is 320 x 240 pixels and the mobile TV watch time goes up to 5 hours. The figure B.1 shows the DVB-H phone N77 that Nokia developed.

Figure B.1: N77 - Nokia DVB-H phone

Some other characteristics:

- DVB-H based mobile TV with internal antenna (470-750 MHz)

- Dedicated TV application for selection, purchase, and consumption of TV programs
- Replay of TV program (up to 30 seconds) and a reminder setting via Program Guide
- Mobile TV interactive services for example voting
- Channel and content protection: OMA DRM2.0, IPsec
- Integrated DVB-H. Video/audio codecs: H.264 AVC 384kbps@QVGA 15fps/QCIF 30fps and AAC up to 128kbps)
- Automatic channel discovery
- Organize channels in your favorite order
- Up to 50 channels (a mix of TV and radio channels) and 5 hours watch time
- Multiple subscription and payment methods (pay TV including previews, free-to-air, pay per view)

Appendix C

Phone position

C.1 For a short time

Pictures for user A (phone held less than 1 minute):

1. Phone held horizontally, a hand on each side of it.
    - Back view: figure C.1
    - Left-side view: figure C.2
    - Top view: figure C.3
2. Phone held vertically, the left hand holding the left side of the phone, and the right hand holding the back of the phone.
    - Back view: figure C.4
    - User view: figure C.5
    - Top view: figure C.6

Pictures for user B (phone held less than 1 minute):

1. Phone held horizontally, a hand on each side of it.
    - Back view: figure C.7

Figure C.1: Horizontally back view

Figure C.2: Horizontally left-side view

Figure C.3: Horizontally top view

Figure C.4: Vertically back view

Figure C.5: Vertically user view

Figure C.6: Vertically top view

- Top view: figure C.8
- User view: figure C.9

2. Phone held vertically, the left hand holding the left side of the phone, and the right hand holding the back of the phone.
   - Back view: figure C.10
   - Left-side view: figure C.11
   - User view: figure C.12

Figure C.7: Horizontally back view

Figure C.8: Horizontally top view

Figure C.9: Horizontally user view

Figure C.10: Vertically back view

Figure C.11: Vertically left-side view

Figure C.12: Vertically user view

C.2 For more than 1 minute till 5 minutes

In the first case, where the user is sitting on a bed, we noticed that the phone is held horizontally with the 2 hands, each one on each side of the phone. This position of the hands lasted 2 minutes. After that the user put instinctively the phone on the bed: so the phone was "laying" on the bed and the user's hands were free. This lasted around 2 minutes as well. Then the user took the phone again but only with his right hand: the fingers were placed on the back of the phone and the thumb was located under the phone. 20 seconds later the user took exactly the same phone position but holding this time the phone with his left hand. After 20 seconds the user put again the phone on the bed till the end of the movie. The experiment lasted 5 minutes (duration of the movie).

In the second case the same user is waiting at a bus stop. We gave him the mobile phone after having set the same movie on it. The user started by holding the phone with his 2 hands, each one on each side of the phone and some fingers located on the back of the phone. 1 minute later only the right hand was holding the phone: all the fingers were holding the back of the phone and the thumb was on the front, down the screen. Again 1 minute later the user held the phone with his 2 hands. And after 2 minutes the experiment stopped.

We notice that when the user has to hold the phone for more than 1 minute, it's difficult for him to keep the same hand position on the phone. This is due to the fact that it's tiring to keep a constant position. So the positions will change.

1. The user is sitting on a bed watching a movie on the mobile phone

Figure C.13: 2 hands holding the phone

Figure C.14: Phone laying on the bed

Figure C.15: Right hand holding the phone

Figure C.16: Left hand holding the phone

- First position: the phone is held with the 2 hands on each side of the phone (figure C.13)
- Second position: the phone is laying on the bed (figure C.14)
- Third position: the phone is held with the right hand (figure C.15)
- Forth position: the phone is held with the left hand (figure C.16)
- The last position is when the phone is laying on the bed again

2. The user is waiting at a bus stop

- First position: the 2 hands are holding the phone (figure C.17)
- Second position: one hand is holding the phone (figure C.18 and figure C.19)

Figure C.17: 2 hands holding the phone at the bus stop

Figure C.18: One view of the right hand holding the phone at the bus stop

Figure C.19: Another view of the right hand holding the phone at the bus stop

Appendix D

Basic solutions for the matching network

A very simple matching network is the L-section, made up by two reactive components (inductors or capacitors), that can match an arbitrary load impedance to a transmission line. Here the very basic solutions of the matching network are presented. There are two possible configurations for this matching network, depending on the value of the load impedance [31]. Defining R_L the resistive part of the load impedance Z_L and X_L its reactive part, and Z_0 the characteristic impedance of the transmission line.

1. If $R_L > Z_0$, the resistive part of the antenna is higher than the one of the transmission part [31]. The load impedance must be equal to Z_0 and the network looks like in figure D.1:

$$Z_0 = jX + \frac{1}{jB + \frac{1}{R_L + jX_L}} \tag{D.1}$$

   Solving the previous equation separating real and imaginary parts we have [31]:

$$B = \frac{X_L \pm \sqrt{\frac{R_L}{Z_0}(R_L^2 + X_L^2 - Z_0 R_L)}}{R_L^2 + X_L^2} \tag{D.2}$$

$$X = \frac{1}{B} + \frac{X_L Z_0}{R_L} - \frac{Z_0}{B R_L} \tag{D.3}$$

   If B is positive, the element in parallel is a capacitor. If B is negative, it is an inductor. If X is positive, the element in series is an inductor. If X is negative, it is a capacitor [31].

2. If $R_L < Z_0$, the load impedance must be equal to Z_0 and the network looks like in figure D.2):

$$Z_0 = \frac{1}{jB + \frac{1}{R_L + j(X + X_L)}} \tag{D.4}$$

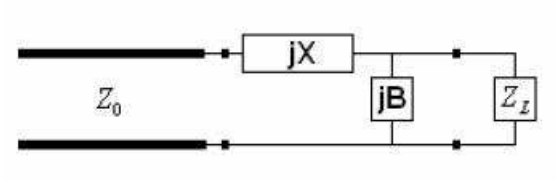

Figure D.1: Matching network for the first case
[31]

Solving the previous equation separating real and imaginary parts we obtain [31]:

$$B = \pm\frac{1}{Z_0}\sqrt{\frac{Z_0 - R_L}{R_L}} \tag{D.5}$$

$$X = \pm\sqrt{R_L(Z_0 - R_L)} - X_L \tag{D.6}$$

If B is positive, the element in parallel is a capacitor. If B is negative, it is an inductor. If X is positive, the element in series is an inductor. If X is negative, it is a capacitor [31].

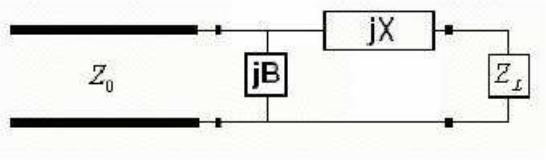

Figure D.2: Matching network for the second case
[31]

For multiple matching circuits for increasing the bandwidth, Chebyshev solutions are normally used [22]: thus it provides a maximum bandwidth for a given maximum reflection coefficient. Chebyshev solutions are presented in Appendix H.

Appendix E

Chebyshev frequency filter design

In this section we will discuss how to design a low pass Chebyshev filter. Then we will use the frequency transformation procedure in order to obtain a bandpass filter.

First, let's normalize the frequency as follows:

$$\omega_{norm} = \frac{\omega}{\omega_c} \tag{E.1}$$

where :

1. ω_{norm} is the normalized pulsation
2. ω is the pulsation ($\omega = 2\pi f$)
3. ω_c is the cut off pulsation

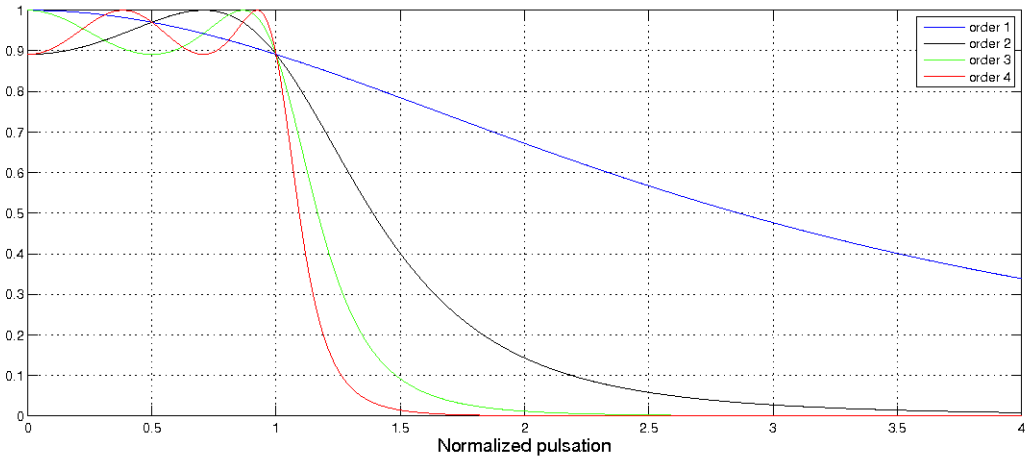

Figure E.1: Chebyshev responses with different orders

The Chebyshev filter approximate the ideal brick-wall response. Contrary to the Butterworth filter that has a more linear phase in the passband, Chebyshev filters are sharper but they show small ripples in the passband. They have the property that they minimize the error between the idealized filter characteristic and the actual over the range of the filter [23].

Figure E.1 shows typical Chebyshev's characteristics with different orders. We can notice that the more the order increases, the faster the slope decreases. The transfer function is derived from the Chebyshev polynomials as shown in equation E.2.

$$|H(j\omega_{norm})|^2 = \frac{H_0}{1 + \varepsilon^2 C_n^2(\omega/\omega_c)} \tag{E.2}$$

where :

1. $C_n^2(\omega)$ is the n^{th}-order Chebyshev polynomial of the first kind
2. ε is the ripple factor that gives a magnitude equal to $\frac{1}{\sqrt{1+\varepsilon^2}}$
3. H_0 is a constant

In order to design a Chebyshev filter, we must choose the design criteria in order to calculate the filter order:

1. α_p is the passband ripple
2. α_s is the stop band attenuation
3. ω_p is the cut off frequency
4. ω_s is the stopband frequency

Then we must calculate the ripple ε that makes the relation between the maximum and the minimum gain in the passband based on α_p. It is determined using the following equations E.3 and E.4:

$$C_n(\omega_{norm}) = cos(n(arcos(\omega_{norm}))) \tag{E.3}$$

$$<=> |C_n(\omega_{norm})| \leq 1 \tag{E.4}$$

for $|C_n(\omega_{norm})| \leq 1$.

Given the equation E.4, the maximum and minimum passband is:

$$max(|H(j\omega_{norm})|^2) = \frac{1}{1 + \varepsilon^2 min(C_n^2(\omega_{norm}))} \tag{E.5}$$

$$= \frac{1}{1+(\varepsilon^2)0} = 1 \text{ for } 0 \leq \omega_{norm} \leq 1$$

$$min(|H(j\omega_{norm})|^2) = \frac{1}{1 + \varepsilon^2 max(C_n^2(\omega_{norm}))} \tag{E.6}$$

$$= \frac{1}{1+(\varepsilon^2)1} = \frac{1}{1+\varepsilon^2} \text{ for } 0 \leq \omega_{norm} \leq 1$$

Then we get $\varepsilon^2 = 10^{\frac{\alpha_p}{10}} - 1$

Now we can determine the order using the stopband requirement. It is normalized as follows: $\omega_{s-norm} = \frac{\omega_s}{\omega_p}\omega_{p-norm}$ where :

1. ω_{s-norm} is the normalized stopband pulsation,

2. ω_{p-norm} is the normalized passband pulsation ,

Then the order n is given by equation E.7:

$$n = \frac{arccos(\sqrt{\frac{10^{\alpha_s/10}-1}{10^{\alpha_p/10}-1}})}{arccos(\omega_{sn})} \tag{E.7}$$

Appendix F

Antennas covering the band 470 MHz - 730 MHz

We would like to present 2 antennas that we simulated in order to show how it is possible to cover the whole band of interest. These 2 antennas are large compared to the one we want to implement in the DVB-H system.

- The first antenna is a monopole with a length of 12cm. The source is between the wire and the brick. The brick's length is 8cm, its width is 4cm and its height is 2cm. Figure F.1 displays the antenna configuration (see figure F.3 for results).
- The second antenna is the big pifa: the length is equal to 3cm, the width is 1cm. It is located at 14 cm from the ground plane which length is 20cm and the width is 15cm. Figure F.2 displays the antenna configuration (see figure F.4 for results).

We notice that with the monopole the whole band of interest. The Pifa results in figure F.4 show that the bandwidth at -3dB covers the frequencies between 560 MHz and 730 MHz.

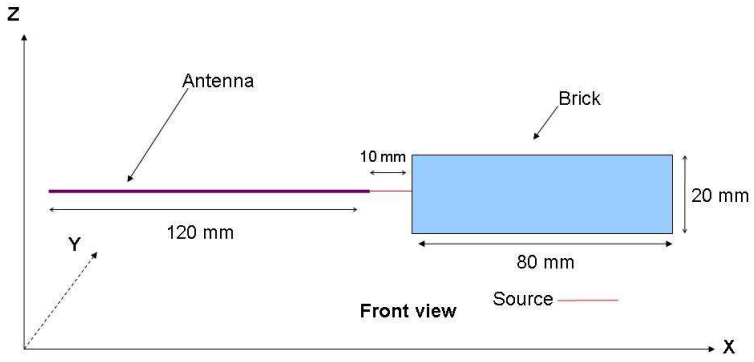

Figure F.1: Monopole antenna

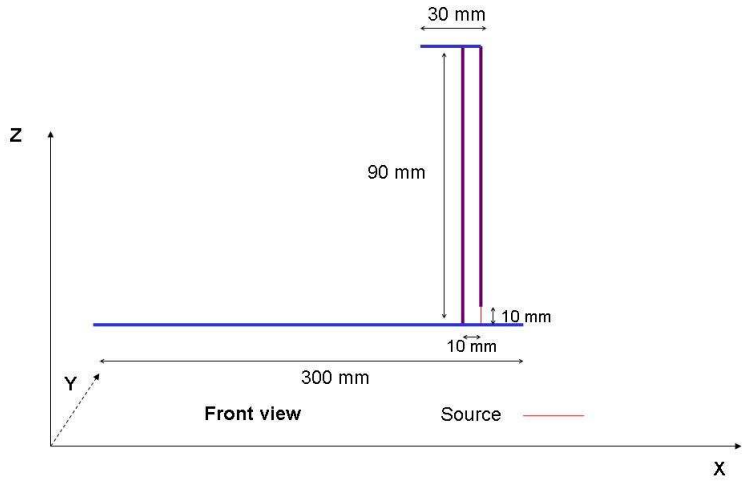

Figure F.2: Pifa antenna

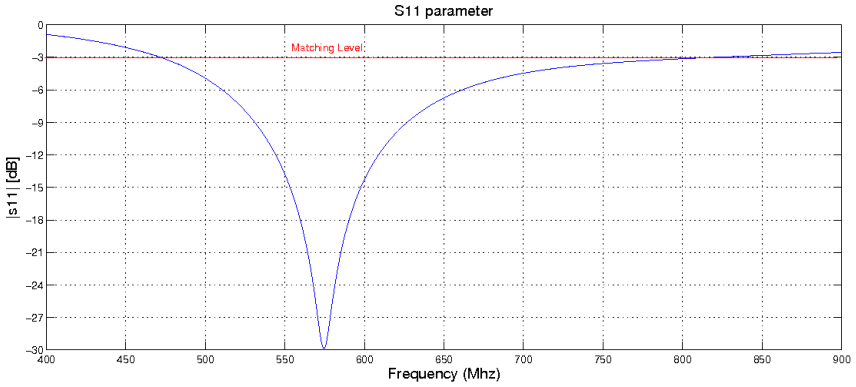

Figure F.3: Monopole antenna

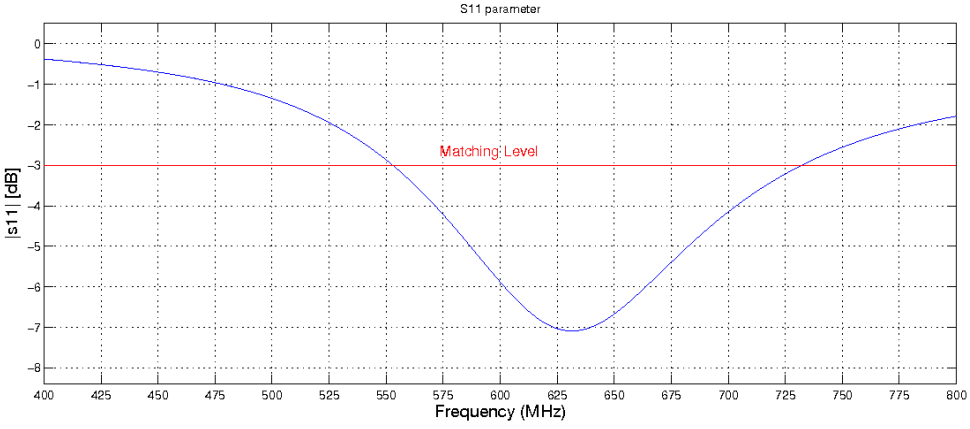

Figure F.4: PIFA antenna

Appendix G

Fredrik and Mattias's loop antenna

Loop antenna as the one presented in figure G.1 has been tried in Fredrik Persson and Mattias Wideheim's master thesis. The loop antenna is then tuned using diodes. We have simulated it with a length of 235 mm. The results we got were not the same as Fredrik and Mattias's results. We needed to get more information about the values of the components they used to try to have the same results. However the size of their antenna was too big so it was not a promising antenna: it cannot be chosen for DVB-H reception in a small device.

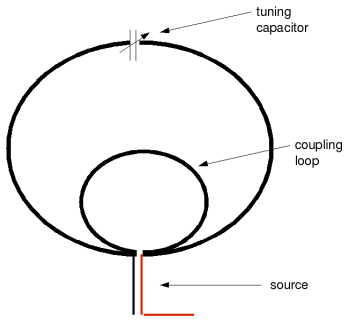

Figure G.1: 3D-Loop antenna

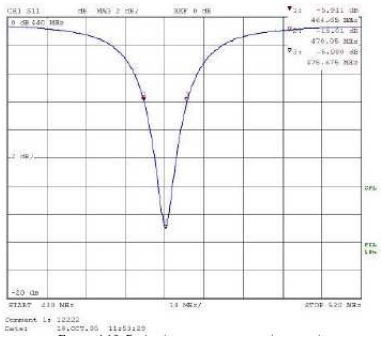

Figure G.2: Loop antenna S11 -Fredrik and Mattias's results

Appendix H

Chebyshev bandpass matching circuit design

This chapiter will discuss how to design a Chebyshev bandpass matching circuit. We have used [25] in order to understand the theory of wideband matching.

The first thing to do is to measure the impedance or admittance characteristics of the resonated load across the frequency band of interest. We note f_1 and f_2 to the edges of the frequency of interest. In ideal cases, the real part of the impedance (or of the admittance) is constant and the imaginary parts have odd symmetry about f_0 . In reality this is not the case when doing wide band matching where the load impedance may deviate from these ideal symmetrical characteristics [26].

We have to choose between the idealized series-resonated load or shunt resonated load to characterize our antenna. If the real part of the antenna's impedance is more constant than the admittance then it looks more like the idealized series resonated load and we calculate R_a and the decrement δ as follows:

$$R_a = Real(Z_l|_{f=f_0}) \tag{H.1}$$

where Z_l is the impedance of the load and f_0 is the central frequency of our band.

$$\delta = \frac{R_a}{|Imag(Z_l)|_{f=f_1 or f_2}} \tag{H.2}$$

Otherwise if the admittance of the antenna is the most constant then it looks like the idealized shunt resonated load and we calculate G_a and the decrement δ as follows:

$$G_a = Real(Y_l|_{f=f_0}) \tag{H.3}$$

where Y_l is the admittance of the load and f_0 is the central frequency of our band.

$$\delta = \frac{G_a}{|Imag(Y_l)|_{f=f_1 or f_2}} \tag{H.4}$$

If the real part of the impedance is the most constant, we add a reactance element in series so as to bring the load to series resonance at f_0, the midband frequency of the frequency range over which a good impedance match is desired. If the real part of the admittance is the most constant, add a reactance element in shunt with the load so as to bring the load to parallel resonance at f_0 [26].

H.1 Low pass prototype parameters

After that we have to select an appropriate low pass prototype filter with the selected δ value. The higher the order, N, of the filter the faster the Chebyshev slope can be achieved as shown in appendix E. It is important to remember that good matching is not possible all over the band. The more a minimum loss for a certain band is achieved, the more it has to be compensated by higher loss for another band. g_0, g_1, g_2,..., g_n, g_{n+1} are the element values as shown in figure H.1.

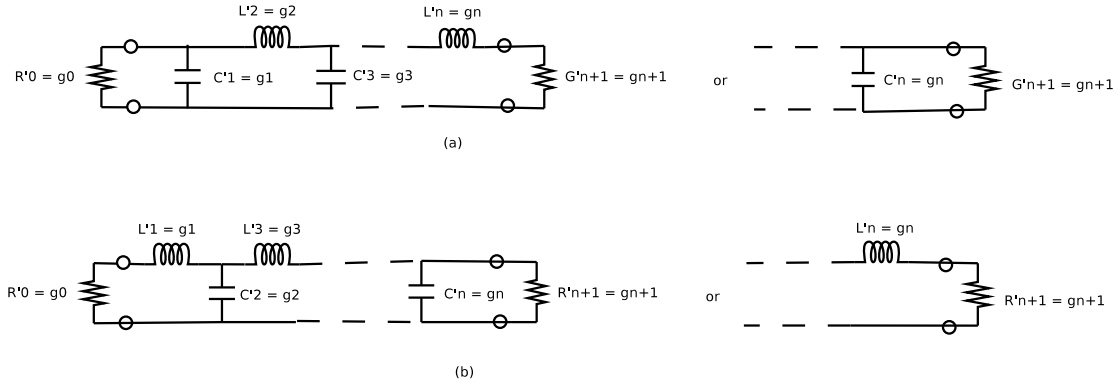

Figure H.1: Definition of prototype filter parameters

The figure H.1 [28] shows a prototype circuit (a) and its dual (b). Either forms may be used since both give identical responses. In this figure, the following conventions are observed:

$g_{k|_{k=1ton}}$ is the inductance of a series coil, or the capacitance of a shunt capacitor.

g_0 is the generator resistance $R_0^{'}$ if $g_1 = C_1^{'}$, but is defined as the generator conductance $G_0^{'}$ if $g_1 = L_1^{'}$.

R_{n+1} is the load resistance $R_{n+1}^{'}$ if $g_n = C_n^{'}$, but is defined as the load conductance $G_{n+1}^{'}$ if $g_n = L_n^{'}$.

Besides the circuit element values, g_k, an additional prototype parameter, $\omega_1^{'}$, will also be used. It is the radian frequency of the pass-band edege. The element values of the prototype filters are all normalized to make $g_0 = 1$, and $\omega_1^{'} = 1$.

Using the formulaes from [27], we calculate the values of the elements for a given L_{Ar} passband ripple in dB, g_0= 1 and $\omega_1^{'}$=1 as follows:

$$\beta = ln\left(coth(\frac{L_{Ar}}{17.37})\right) \tag{H.5}$$

$$\lambda = sinh\left(\frac{\beta}{2N}\right) \tag{H.6}$$

$$a_k = sin\left(\frac{(2k-1)\pi}{2n}\right), \tag{H.7}$$

where k= 1,2,...,n.

$$b_k = \lambda^2 + sin^2\left(\frac{k\pi}{n}\right), \tag{H.8}$$

where k= 1,2,...,n. Then we compute:

$$g_1 = \frac{2a_1}{\lambda} \tag{H.9}$$

$$g_k = \frac{4a_{k-1}a_k}{b_{k-1}g_{k-1}} \tag{H.10}$$

$$g_{N+1} = 1 \tag{H.11}$$

for N odd,

$$g_{N+1} = coth^2\left(\frac{\beta}{4}\right) \tag{H.12}$$

for N even;

H.2 Lowpass to bandpass conversion

Once the g_k elements have been calculated, we must make the lowpass to bandpass conversion. We will do it using the method from [28]. We first define the $\omega^{'}$, ω_0, ω_1, ω_2 , the fractional bandwidth ω_b such as:

$$\frac{\omega^{'}}{\omega_1^{'}} = |\frac{2 - \frac{\omega_0}{\omega} - \frac{1}{2-\frac{\omega_0}{\omega}}}{2 - \frac{\omega_0}{\omega_2} - \frac{1}{2-\frac{\omega_0}{\omega_2}}}| \tag{H.13}$$

where

$$\omega_0 = \omega_1 + \omega_2 - \sqrt{\left(\omega_2 - \omega_1\right)^2 + \omega_1\omega_2} \tag{H.14}$$

$$\omega_1 = 2\pi f1 \tag{H.15}$$

$$\omega_2 = 2\pi f2 \tag{H.16}$$

$$\omega_b = \left(\frac{\omega_0}{\omega_1} - \frac{\omega_0}{\omega_2}\right) \tag{H.17}$$

Then we must choose the values of R_a (the real part of the impedance at f_0), R_b which is the load to match and L_{r0}, L_{r1},..., L_{rN}, L_{rN+1} where N is the order of the filter and the L_{rj} are related to the L_{pj} as indicated in the equations below:

$$L_{p0} = L_{r0} \tag{H.18}$$

$$L_{p1} = L_{r1} + M_{01} - M_{01}^e \tag{H.19}$$

$$L_{pj}|_{j=2toN-1} = L_{rj} \tag{H.20}$$

$$L_{pN} = L_{rN} + M_{N,N+1} - M_{N,N+1}^e \tag{H.21}$$

$$L_{pN+1} = L_{rN+1} \tag{H.22}$$

where

$$M_{01}^e = \frac{M_{01} + \frac{(L_{r0}-M_{01})\omega_0^2 M_{01}L_{p0}}{R_a^2}}{1 + \left(\frac{\omega_0 L_{r0}}{R_a}\right)^2} \tag{H.23}$$

$$M^e_{N,N+1} = \frac{M_{N,N+1} + \frac{\left(L_{rN+1} - M_{N,N+1}\right)\omega_0^2 M_{N,N+1} L_{pN+1}}{R_b^2}}{1 + \left(\frac{\omega_0 L_{rN+1}}{R_b}\right)^2} \tag{H.24}$$

And the capacitors:

$$C_{rj}|_{j=1toN} = \frac{1}{L_{rj}\omega_0^2} \tag{H.25}$$

$$K_{01} = \sqrt{\frac{R_a \omega_0 L_{r1} \omega_b}{g_0 g_1 \omega_1^{'}}} \tag{H.26}$$

$$K_{j,j+1}|_{j=1toN} = \frac{\omega_b \omega_0}{\omega_1^{'}} \sqrt{\frac{L_{rj} L_{rj+1}}{g_j g_{j+1}}} \tag{H.27}$$

$$K_{N,N+1} = \sqrt{\frac{R_b \omega_0 L_{rN} \omega_b}{g_N g_{N+1} \omega_1^{'}}} \tag{H.28}$$

The mutual couplings are:

$$M_{01} = \frac{K_{01}}{\omega_0} \sqrt{1 + \left(\frac{\omega_0 L_{r0}}{R_a}\right)^2} \tag{H.29}$$

$$M_{j,j+1}|_{j=1toN-1} = \frac{K_{j,j+1}}{\omega_0} \tag{H.30}$$

$$M_{N,N+1} = \frac{K_{N,N+1}}{\omega_0} \sqrt{1 + \left(\frac{\omega_0 L_{rN+1}}{R_b}\right)^2} \tag{H.31}$$

The series inductances are :

$$L_0 = L_{r0} - M_{01} \tag{H.32}$$

$$L_1 = L_{r1} - M^e_{01} - M_{12} \tag{H.33}$$

$$L_j|_{j=2toN-1} = L_{r1} - M^e_{01} - M_{12} \tag{H.34}$$

$$L_N = L_{rN} - M_{N-1,N} - M^e_{N,N+1} \tag{H.35}$$

$$L_{N+1} = L_{rN+1} - M_{N,N+1} \tag{H.36}$$

The figure H.2 shows the lowpass prototype while figure H.3 shows the bandpass prototype. The figure H.4 shows bandpass matching circuit with the serie reactance element to bring the load to series resonance at f_0.

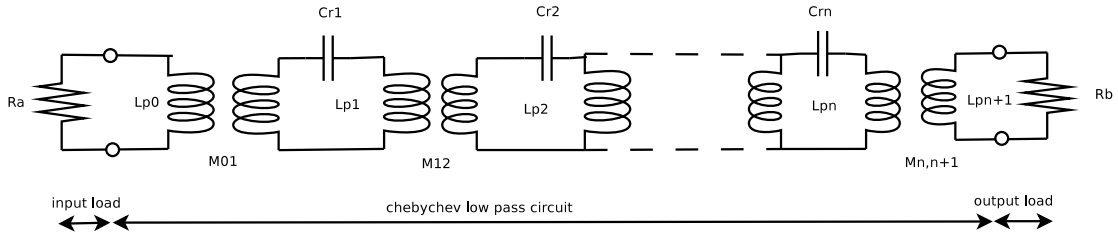

Figure H.2: Chebyshev lowpass prototype

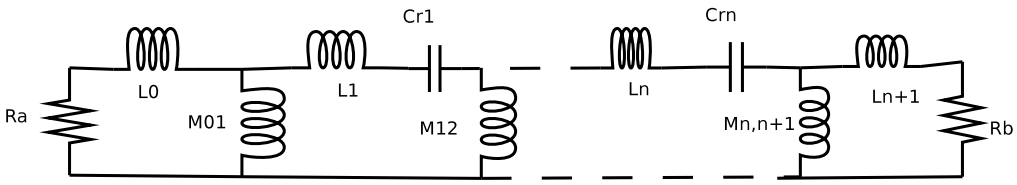

Figure H.3: Chebyshev bandpass prototype

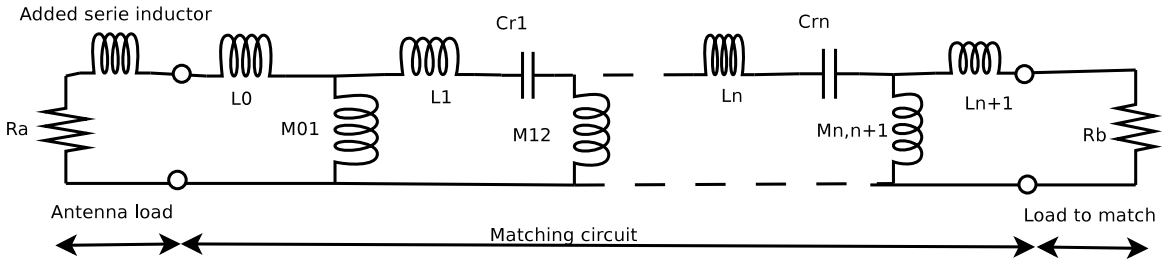

Figure H.4: Chebyshev bandpass prototype with serie's reactance

H.2.1 Example of a second order impedance matching circuit

In this section we are going to design a second order impedance matching circuit using the method described in the previous section. For a better comprehension, we will assume that the impedance of our antenna is constant and equal to 12 + 36i at any frequency. Futhermore the impedance to match will be 50 ohms over the band 470 - 730 Mhz and the choosen Lar will equal to 2 dB. Finally we define all the Lr values equal to 10^{-9} to have components values of the good order.

Using the previous information we can define :

- f1 = 470 Mhz, f2= 730 Mhz and so ω_1 and ω_2,
- $R_a = 12$ and $R_b = 50$,
- N =2.

From equations H.5 to H.12 we obtain the following values:

- $\beta = 2.1660$
- $\lambda = 0.5684$
- g_0=1, g_1=2.4883, g_2=0.6075, g_3=1.

Then it is possible to calculate the L, M and Cr values from equations H.13 to H.36 and obtain:

- L_0= 0.199 nH, L_1= -0.338 nH, L_2= -2.698 nH, L_3= -2.160 nH.
- Cr_1= 67.13 pF, Cr_2= 67.13 pF.
- M_{01}= 0.801 nH, M_{12}= 0.597 nH, M_{23} = 3.160 nH.

It is important to notice that the value of L_1, L_2 and L_3 are negative values. In some cases, using the model proposed before leads to unrealizable circuits. A solution would be to replace the "negative" coils by capacitors. But doing this will change the response in the frequency domain. It could be a solution only for a given frequency. The figure H.5 presents reflection coefficient in function of the frequency. It has been plotted by calculating the equivalent resistance of the realized circuit Z_e and then using the equation 2.3.

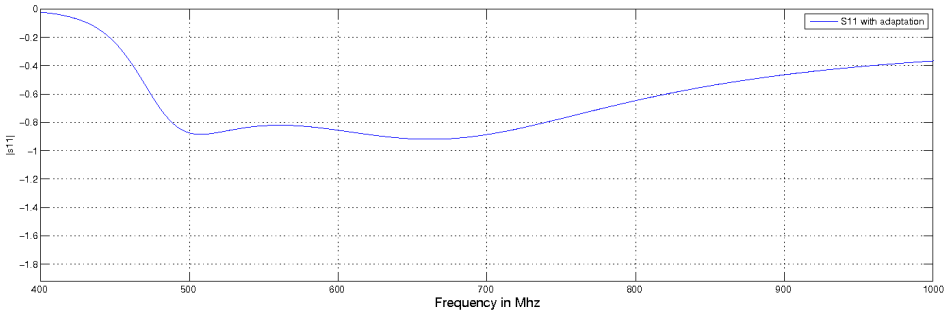

Figure H.5: S11 response using the prototype parameters of the example

Appendix I

Matlab code

Behind this page, you will find our Matlab code.